IMAGE QUALITY AND LESION DETECTION IN MAMMOGRAPHY: A COMPARATIVE STUDY BETWEEN FULL-FIELD DIGITAL MAMMOGRAPHY AND COMPUTED RADIOGRAPHY DIGITAL MAMMOGRAPHY

BY

DESMOND BEDIAKO

(10876873)

THIS THESIS IS SUBMITTED TO THE UNIVERSITY OF GHANA, LEGON IN PARTIAL FULFILMENT OF THE REQUIREMENT FOR THE AWARD OF MPHIL IN MEDICAL PHYSICS DEGREE

DECEMBER, 2022

DECLARATION

Candidate's Declaration

I hereby declare that this thesis is a sole result of my personal and original research and no aspect of this work has been submitted to the University of Ghana for another degree or presented elsewhere for any other purposes.

Candidate's Signature: …… Date: 13-06-2023

Name: **Desmond Bediako**

Supervisor's Declaration

We declare that the planning, execution and presentation of this thesis were supervised in strict guidance of supervision adhered to by the University of Ghana.

Principal Supervisor's Signature: …… Date: 13th June, 2023

Name: **Dr Edem Kobla Sosu**

Co - Supervisor's Signature: …… Date: 13-06-2023

Name: **Professor Mary Boadu**

ABSTRACT

Image quality and lesion detection abilities are primary to accurate diagnosis in medical imaging; hence this study was aimed at examining the image quality and lesion detection abilities in Full-Field digital mammography and Computed Radiography digital mammography using the American College of Radiology Mammography Accreditation Phantom (ACR-MAP). Pre-exposure and exposure tests were conducted to establish the effective performance of the mammography systems used. DICOM images were obtained of the ACR-MAP at varying values mAs and kVp. Qualitative image quality assessment was made using the internationally recommended protocol for detection scoring. Quantitative image quality was also estimated using the ImageJ software and the Albert Rose Model to analyze image quality with reference to the Human Health Series numbers 2 and 17 of the International Atomic Energy Agency (HHS - IAEA). Results of the pre-exposure and exposure texts showed optimal and satisfactory performance of four of the systems. The half value layer result of the system D within the CRDM systems was below the recommended limit; hence the poor quality and detection exhibited by the machine of that facility. The obtained signal-to-noise ratio (SNR) and spatial resolution results indicated standard quality images were achievable at the 20 mm and 45 mm thicknesses within both systems but poor-quality images at 70 mm. Signal-to-noise ratio and spatial resolution decreased with increasing PMMA thickness. SNR was 16 % more in FFDM than that of CRDM, whiles the spatial resolution was 0.5 lp/mm, 1.0 lp/mm and 0.5 lp/mm more in in the FFDM systems compared to the CRDM systems within the respective PMMA thicknesses, indicating adequate quality within FFDM. Both FFDM and CRDM systems produced quality images proportional to increasing the detectability as the technique factors (kVp and mAs) increased with the ACR MAP, with the FFDM system's average percent visibility at 89.05 % and that of CRDM at 75.00 %. The FFDM proved superiority in image quality and lesion detection over the CRDM.

ACKNOWLEDGEMENTS

I am extremely thankful to God Almighty for His enabling strength, provisions and safety granted me throughout the period of my study and the execution of this work. I am sincerely grateful to my supervisors; Dr. Edem K. Sosu and Prof. Mary Boadu, for their continued inputs of directions, guidance and corrections throughout this work. I like to acknowledge the immediate past Head of Department, Prof. Francis Hasford, and the entire staff of the Medical Physics Department most especially Dr. Theresa Dery for their immense contributions and support throughout my study period in the department.

My heartfelt appreciation goes to my uncle Dr. Winfred K. Kokor for his financial support on regular and timely basis. To my sweet mother, Madam Rose Kokor, I am deeply grateful to you for your love and constant encouragement and words of counsel, God bless you.

I also wish to extend my appreciation to WO1(Rtd) George Bediako and his wife for hosting me throughout the period. To my siblings, Racheal, Kingsley and Godfred, I am utterly amazed by your individual contributions to this journey, I thank you.

GOD BLESS YOU ALL

DEDICATION

To my beloved mother, Madam Rose Korkor

TABLE OF CONTENTS

LIST OF TABLES

LIST OF FIGURES

LIST OF ACRONYMS

ACR-MAP - American College of Radiology Mammography Accreditation Phantom

AEC - Automatic Exposure Control

CC – Cranio-Caudal

COV - Coefficient of Variation

CR - Computed radiology

CRDM - Computed Radiology Digital Mammography

CT - Computed Tomography

DCIS - Ductal Carcinoma In-Situ

DICOM - Digital Imaging and Communication in Medicine

DQE - Detective Quantum Efficiency

FFDM - Full-Field Digital Mammography

FITS – Flexible Image Transport System

GIF – Graphics Interchange Format

HHS – Human Health Series

HVL - Half Value Layer

IAEA – International Atomic Energy Agency

ICRP – International Commission on Radiological Protection

JPEG – Joint Photographic Expects Group

kVp - X-ray Tube Voltage

mAs - X-ray Tube Output

MLO - Medial-Lateral Oblique

Mo/Mo – Molybdenum/Molybdenum

Mo/Rh - Molybdenum/Rhodium

MRI - Magnetic Resonance Imaging

MTF - Modulation Transfer Function

NEMA - National Electrical Manufacturers Association

PACS - Picture Archiving and Communication System

PMMA – Polymethyl Methacrylate

PSP - Photostimulable Phosphor

QC - Quality control

Rh/Al - Rhodium/Aluminum

Rh/Rh - Rhodium/Rhodium

ROI - Region of Interest

SNR – Signal-to-Noise Ratio

TIFF – Tag Image File Format

USB - Universal Serial Bus

W/Rh - Tungsten/Rhodium

CHAPTER ONE

INTRODUCTION

1.1 Background

Breast cancer is a tumor often originating from the glandular tissues in the female breast. The disease is fatal, and the most frequently diagnosed disease or cancer prevalent in women, and the commonest cancer that is associated with mortality among women (DeSantis *et al.*, 2017). In Ghanaian women, the disease is a very familiar malignant disease resulting in the bulk of deaths related to cancer (Wiredu & Armah, 2006). Unfortunately, reports or data on the disease in Ghana are inadequate (Biritwum & Amaning, 2000). In Ghana and in the sub-Saharan African region, the generality of the disease among black African women is often acute with critical features (Wiredu & Armah, 2006) due to the late presentation to the health care professionals and inadequate screening and therapeutic interventions. The disease has over the years been of concern to stakeholders and a public health challenge whose prevention remains a major problem because the cause is still unclear to researchers (Laprovitera *et al.*, 2021). At the early stage of breast cancer, there are usually no symptoms and is most often noticed or diagnosed through breast self-examination, clinical breast examination and mammography screening and other imaging modalities.

When the disease gets to a more severe stage, then the symptoms begin to manifest. The commonest symptom is a pain-free lump in the breast. Other indicators of the disease includes but are not limited to the following: continuous variations in the breast, such as stiffening, enlargement, and nipple deformity like intermittent discharges or retractions (ACR, 2019). In the beginning stages of breast cancer development, the infected cells separate themselves from each other extending to other regions of the breast implicating dire complications if not detected and

managed at these early stages. However, the accurate diagnosis of breast cancer at an early stage can increase the possibility of treatment and total recovery and reduce the probability of recurrence and mortality rate. In recent times, there is evidence of decrease in breast cancer death rate in some developed countries and this milestone is attributed to early detection through screening schemes and timely and potent diagnosis and treatment protocols (Weir *et al.*, 2003). This same narrative may not apply to Ghana and the sub-Saharan African region due to the inadequacy of these screening schemes and quality cancer care (Mensah *et al.*, 2016).

Mammography is a radiographic (X-ray) procedure optimized for the examination of the breast; it has a very high ability to detect early-stage breast cancer (lesions). Mammography has become an extremely accepted and useful non-invasive imaging modality with unmatched capabilities of lesion and microcalcification detection in the breast (ACR, 2019). A predominant target of screening mammography is its ability to detect the radiological masses (lesions) in the breast at a fairly early-stage such that ensuring treatment will reduce the possibility of death (Yaffe *et al.*, 2013).

However, just like any measuring or screening tool, mammography is not 100% perfect (ACS, 2020), it is hence highly expected that the mammography system exhibits excellent responsiveness to lesions in order are not to overlook lesions (false negative). But to achieve this feat, equipment performance and exposure parameters (technique factors) must be selected with the quality of the image and the expected detection task as priorities and ensuring that the patient's absorbed dose is kept as low as reasonably achievable (ACR, 2019). The screening of breast cancer using X-ray mammography is highly beneficial if the modality can detect breast cancers (lesions) at an early stage. This can be made possible with high-quality breast images (mammograms) to ensure the possible detection of the smallest lesions in the breast (Yaffe & Mainprize, 2011). Ultimately, the

most relevant aim regarding mammography systems is the unwavering ability of providing contrast amidst a lesion possibly occupying a region in the breast and the uninfected tissues in the same region in the breast (Chevalier *et al.*, 2012). The intentional screening mammography programs continuously contribute immensely to guarding women within certain ages and who are uncertain due to their respective family history to the disease. Thus, the quality of mammograms is given equal importance if not more since the ability to detect lesion is directly proportional to the quality of mammograms (Yaffe & Mainprize, 2011).

Mammography image quality emphasizes the system's ability in visualizing the anatomy of the breast sufficiently, mainly depicting the internal structures of the breast (Thevi *et al.*, 2012). A primary goal of quality control and optimization in mammography is to better the detection of microcalcifications and lesions originating from and residing in breasts. In a quantitative approach, the image quality can be measured using parameters such as spatial resolution, artefacts, noise and signal-to-noise ratio. The criteria used in diagnostic radiography for image quality in mammography addresses the standard required for image quality (Samei *et al.*, 2005). Image quality analysis is done with reference to only a particular imaging mandate. Notwithstanding, the main image quality requirements most important in radiography are image contrast, noise, sharpness; these features are equally relevant in mammography. Considering the evolutions in technology and imaging of the breast, a matching level of image quality is required with respect to the necessary parameters. This study will specifically focus on the ability of the mammography system in detecting masses in the breast with similar optical densities with reference to high signal-to-noise ratio which are commonly defined for mammography equipment with variation, depending on the manufacturer and the system specifications (Thevi *et al.*, 2012).

1.2 Statement of the Research Problem

Lesions and microcalcifications are the most important finding in asymptomatic patients with early breast cancer. The early detection of cancer using mammography highly reduces the risk of death and increases treatment options. Breast cancer detection in mammography is often challenged by the difficulty to differentiate between breast tissues and other pathological findings which appear to have almost the same or close linear attenuation in the energy range used in mammography. Moreover, the seeming imperfections in mammography may result in missing the detection of cancer (false negative). The rise in false-positive and high false-negative detection rates in mammography can largely be linked to the poor quality of mammograms leading to the difficulty in the differentiation of lesions and the anatomical background.

In Ghana, an estimated 10% of positive breast cancers cases missed in mammography examination (Dzidzornu *et al.*, 2021) basically due to poor image quality. The widely accepted confidence in digital systems to produce maximum quality images is unmatched, yet there exists the potential of non-detection of breast cancer even by the virtue of digital imaging modalities. Important parameters that determine image quality and lesion detectability in mammography are noise, (spatial fluctuation), artefacts and signal-to-noise. These parameters help improve diagnostic accuracy while reducing accumulative radiation exposure to unsuspecting women. This work will assess the major parameters used in mammography and their respective effects on image quality and lesion detection abilities.

1.3 Objectives

The primary aim of this study was to examine the image quality and lesion detection in the Full-Field Digital Mammography (FFDM) and Computed Radiology Digital Mammography (CRDM).

The specific objectives of the study were to:

1. compare the pre-exposure and exposure performance between the two modalities;
2. assess the qualitative image quality at varying exposures between the two modalities;
3. assess the quantitative image quality at varying exposures between the two modalities.

1.4 Relevance and Justification

A major aim of mammography is the ability to commence the treatment as early as the lesions are detected hence reducing the rate of breast cancer deaths that may occur as a result late detection or late start of treatment of the disease at far-advanced stages (Yaffe *et al.*, 2013). The need to optimize the exposure factors on the mammography system is highly necessary for the enhancement of image quality, noting the relevance of higher contrast techniques and their effect on the detection of a shallow contrast lesions. The need to determine how well modern mammography machines can distinguish between possible tiny lesions and normal tissues requires maximum confidence in the quality of images produced by digital systems. A small number of studies also acknowledges the impact of high noise on the detection of infections residing in soft tissue with reference to minimized dose to the patient hence keeping exposures as low as reasonably achievable. The ICRP report number 103 (ACR, 2019) recommendation considers the breast as a radiosensitive and vulnerable organ with the breast glandular tissue having a tissue-weighting factor of 0.12, making it important for quality control routines to be consistent in enhancing the adequate performance of the digital systems. It is also important to adhere to other conditions/parameters necessary for maximum performance in digital mammography. The relative decrease in the number of death of women linked to breast cancer due to reliable screening protocols is closely merited to the ability to detect microcalcifications or lesions early. It is however crucial to quantify the detection rate of small masses and lesions in full-field digital

mammography system and compare its abilities to that of computed radiology digital mammography, hence substantiating the superior imaging modality or technique for scheduled screening programs for breast cancer. The enthusiasm to reduce the occurrence of high false negative and high false positive mammograms is an important justification for the comparative study between the traditional computed radiology digital mammography and the full-field digital mammography systems.

1.5 Scope and Limitation

This study was phantom-based, conducted in five mammography centers within the Greater Accra region, Ghana.

1.6 Organization of the study

This investigative work is reported in chronological order of five chapters. Chapter one gives a broad overview to the study topic, the chapter also introduces the statement of the research problem and description of the main problems addressed in the study. Chapter two reviews the existing literature and relevant research associated with the problem of this study. Chapter three presents and focuses on the materials and methods employed for the collection of relevant data and their respective analysis to ensure successful image quality and lesion detection assessment. The data analysis and its results presentation are indicated in chapter four, whereas chapter five offers the needed summary and related discussion of findings, their implications to everyday practice or clinical implementation, the conclusion, recommendations and suggestions for future research.

CHAPTER TWO

LITERATURE REVIEW

2.1 Introduction

Mammography is an examination of the breast using X-rays of relatively low energies. Using mammography for screening aids in the ease of detecting microcalcifications and lesions. In this section, the relevant literature on the subject is reviewed. These include the general knowledge of the female breast, breast cancer, mammography, Computed Radiology Digital Mammography (CRDM), Full-Field Digital Mammography (FFDM), and the general comparisons of image quality and lesion detection abilities between CRDM and FFDM.

2.2 The Female Breast

The breast (Figure 2.1), is such a crucial organ in the human body and contributes immensely to the growth and development of an infant (Mother and Child, 2019). It is seated on an area of the chest wall of the human body. Women as well as men have breasts, but the breast is most often well developed and more useful in women/females. The breast is a gland mostly made up of lobes positioned all over the nipple. The breast produces milk for providing food and nutrition to the baby (Boquien, 2018). Understanding the healthy anatomy and function of the female breasts will help the ease of detecting abnormalities. The tissues of the human/female breast start to develop as early as the fifth to the sixth week of expected infant stages (Bland & Copeland, 1993; Hopkin's, 2020). Often, the aggregate of fatty tissues in the breast determines its size (Mayor Clinic 2020; WMMC 2018). Hence, the size and shape of women's breasts may vary as a result of genetics, diet and ethnicity, and the age of the woman (Pierce *et al.*, 2002). The majority of the volume in the breast is confined to the upper surface part which is often compromised during breast cancer

(Adesunkanmi *et al.*, 2006; Lambe *et al.*, 1994), making that region the common region of tumors in the breast. Though the structure of the male breast seems identical to the female's, the male breast does not possess the needed or special structures for milk production requirements. The breast is made up of special tissues for a specific physiological purpose as milk production, combination, and the discharge of milk (Hassiotou & Geddes, 2013). These functions are performed by the network of hormones and other relevant factors that control the production of milk. Within the four segments of the breast are 15 to 20 lobes specifically for the production of milk, these lobes are opened to the nipple (Pandya & Moore, 2011; Zucca-Matthes *et al.*, 2016). The smaller structures within the lobes are the lobules.

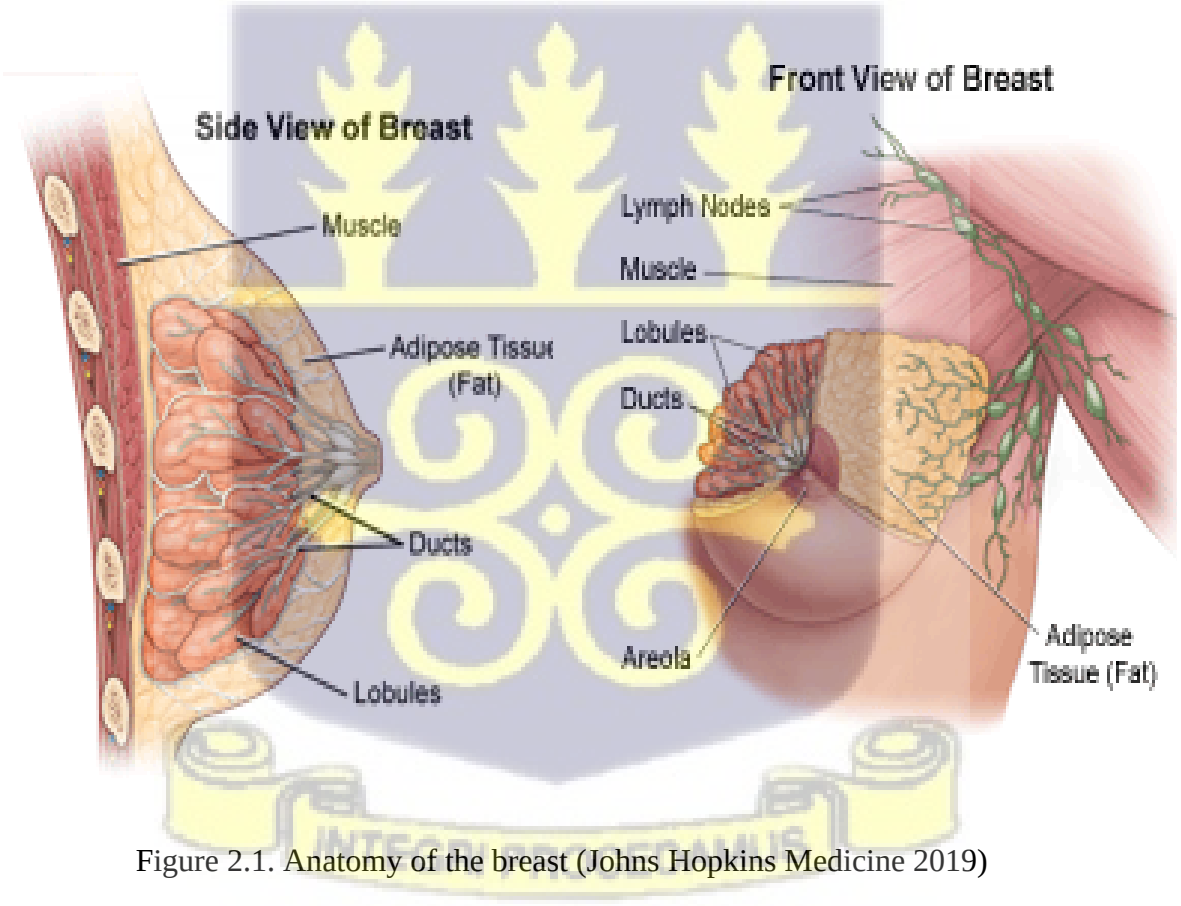

Figure 2.1. Anatomy of the breast (Johns Hopkins Medicine 2019)

Just like other organs in the various systems of humans, the breast and its connecting systems change gradually from birth to adolescence, the menstrual cycle, through pregnancy and lactation.

These changes in the breast are so distinctive since no other organ in the body changes as much in function, shape and size. It is however very crucial to understand the anatomy of the breast and its conduct and response to radiation and imaging modalities.

2.3 Breast Cancer

Breast cancer is a heterogeneous disease caused by the amassing of genetic anomalies, such as regional alterations, displacements/dislocations, and reprinting (Sabel, 2009). Simply put, when cells that make up the breast grow abnormally forming lumps. Breast cancer originates from such abnormal breast cells. Usually, these defects are formed in the ducts which transport produced milk to the nipple. Breast cancer occurs not only in women but also in men, although breast cancer in men is sparse (Anderson *et al.*, 2010; Gethins, 2012; Kreiter *et al.*, 2014). Its impact on the health of women on the other hand is dire, making the disease a key public health challenge for women all over the world (Ghoncheh *et al.*, 2016), resulting in frequent/high deaths among women (Ferlay *et al.*, 2015; Fidler *et al.*, 2017; Wiredu & Armah, 2006). At the pre-malignant lesion or non-invasive stage of the disease, it is contained in the ducts without spreading to other breast tissues that are healthy whiles invasive breast cancer has already outspread beyond or outside the ducts to other good breast tissues, alternatively beyond the breast to lymph nodes or other organs. Breast cancers, just like any other malignancy, are known to spread through the continuous pilling up of several changes in the genetic track controlling enlargement, death, gene repair, and rapid responses to therapy in the neural region (Campbell & Polyak, 2007; Pelengaris *et al.*, 2002). Since the mortality reached its peak value in 1989, the breast cancer death rate in women had declined by some 41% in 2018 due to earlier detection through screening and increased awareness and education on symptoms and the advancement in treatment, bringing the pace of decline to as low as 1% per year (2013 to 2018) compared to the nearly 2% during the 2000s (ACS, 2022).

Worldwide cancer statistics in recent times indicate a rising incidence of breast cancer and the increase among African developing countries including Ghana is at a faster rate than the low incidence rate recorded some years back (Ohene-Yeboah & Adjei, 2012). Some studies have shown the late state at which the patients they seek healthcare whiles cancer may already be at an advanced stage not belittling the menace by poor or lack of diagnostic expertise in the high incidence rate in these developing countries like Ghana. In Ghana, data on the disease is scanty but it is the particular disease with the most incidence in Ghana (Wiredu & Armah, 2006). It is however worrying that the mean age at the stage of breast cancer diagnosis amongst Ghanaian women is 46 years ranging from 26 to 80 years (Ohene-Yeboah & Adjei, 2012) relative to that of over 62 years in other parts of the world (ACS, 2022). The early diagnosis of the disease can increase the rate or chance of early detection and improve survival rates (WHO, 2004). Mammography is however the known most efficient screening tool for detecting breast cancer as early as possible.

2.4 Symptoms of Breast Cancer

Though there is a slight decline in breast cancer incidence worldwide as a result of major factors including early detection (Parkin & Fernández, 2006), it is highly advisable to visit your healthcare provider as early as possible if you experience any changes in your breast or on condition of any of the below-listed symptoms. It is worth noting that these symptoms could reflect other health states though they may be that of breast cancer. Signs such as swelling under the armpit or around the collarbone may be a symptom of a lymph node lump. However, you should discuss any concerns with your doctor. Breast cancer symptoms may largely involve but are not limited to the following: a lump or mass in the breast, changing breast dimensions, rash on the nipple, hollowing of the skin, swelling in the armpit, discharge from the nipple, consistent aches in the breast (CDC

Breast Cancer, 2022) and so on. Nonetheless, the symptoms may sometimes differ and some patients may not even exhibit any signs, hence the need for regular screening.

2.5 Risk Factors/Causes of Breast Cancer

To date, scientists and researchers have not proven a particular cause of breast cancer (Delen *et al.*, 2005). However, multiple factors seem to be linked with a higher risk of developing the disease. It is important to note that as common to almost every form of the disease, exhibiting risk factors does not necessarily mean you have or would have the disease and on the other hand, not also showing these risk factors does not mean one will not get the disease. Most of such factors bear a considerable surge in risk for the woman (Trickey *et al.*, 2012). Old age and sex are the only risk factors for women who make up about 50% of those with the disease, according to literature (Madigan *et al.*, 1995; Renganathan *et al.*, 2014). Over the years, the control and reduction in many of the most delegated risk factors of the disease have not and cannot be controlled by any human intervention (Sosu, 2018). These risk factors include but are not limited to the following.

2.5.1 Gender

Since breast cancer is predominantly woman-related cancer, being born a woman is a major risk factor for breast cancer (ACS, 2022) since the woman's breast undergoes a series of changes and contains more hormones (Armstrong *et al.*, 2000). Men also do get the disease as a result of increased levels of estrogen and androgen, but the disease is more common in women relative to men (Giordano *et al.*, 2002).

2.5.2 Age

The risk of most cancers increases with the increase in age, thus beyond sex, age is a crucial risk factor for breast cancer. This is due to the relationship between the increasing rate of breast cancer amongst the slightly aged (ACS, 2022) since breast cancer is extremely uncommon in women below 30 years. Over 80% of breast cancer-related deaths in other parts of the world were recorded in females above the ages of 40 and 60 years (Coughlin, 2019).

2.5.3 Breast Cancer History

A woman who is diagnosed with breast cancer in one breast has a higher risk and an increased likelihood of developing an all-new infection of the disease in the supplementary breast or other regions of the same breast (Breastcancer.org, 2022). This may differ from regenerated cancer, the risk associated with this is so low in general but maybe so high in younger women with or treated with cancer.

2.5.4 Race/Ethnicity

Though the difference is quickly closing up in recent times, there is however still existing disparities indicating that light skin women develop breast cancer at a higher rate compared to black women. Yet black women are also more prone to die from the disease at random ages due to the prevalence of the triple-negative form of the disease in black women, a more severe form relative to the other forms (Breastcancer.org 2022). It is long confirmed that women except Africans and Asians are seemingly more vulnerable to developing cancer of the breast yet African/black women are more exposed to developing other aggressive and slightly advanced forms of breast cancer likely diagnosed at young ages (Hirko *et al.*, 2022).

2.5.5 Height

Various existing studies show that women who are highly endowed with height (taller) are at higher risk of breast cancer than short women (Kabat *et al.*, 2015; Willett *et al.*, 2014), basically as a result of nutrition in the early stages of life, hormonal or genetic factors. This risk factor can also be related to the growth shoot tall women may have had in their childhood through adolescence from higher levels of hormones and other growth indicators (van den Brandt *et al.*, 2021).

2.5.6 Denser Breast

The breast is composed of fat tissues, fibrous tissues, and glandular tissues. If the breast appears denser on a mammogram, this means the breast has more glandular and fibrous tissue but fewer fat tissues (CDC Breast Cancer, 2022). It is normal to have dense breasts, but in dense breast tissues, it can very difficult to detect or see lesions/cancers on a mammogram. Women who have dense breasts on a mammogram are at high risk of breast cancer compared to women with average breast density though it is not clear if lowering the density of the breast decreases the risk of the disease (Pandya & Moore, 2011; WMMC, 2018).

2.5.7 Early menstrual periods and later menopause

Starting menstrual periods so early increases the woman's risk of developing the disease. In effect, these women turn to have more menstrual cycles compared to other women because they started menstruating so early and they are slightly at higher risk of breast cancer than the others (Eaton, 2002). This increase in the risk can be attributed to a longer period/lasting exposure to the estrogen and progesterone hormones. When the onset of a woman's menstrual cycle starts earlier than it is

supposed to, this results also in the extension of menopause thus cancer risk of those women who go through menopause at older ages increases (Breastcancer.org, 2022).

2.5.8 Overweight

Women who are overweight and obese are at higher risk of breast cancer compared to women who maintain a healthy weight, most importantly after menopause (Picon-Ruiz *et al.*, 2017). Overweight/obese expressed in terms of the individual's body mass index concerning many studies show that being overweight increases the risk of breast cancer redeveloping in women who have been diagnosed with the disease some time passed due to the continuous production of estrogen. Extra fatty cells replicate more estrogen in the body, and estrogen can make hormone receptor-positive breast cancers develop and grow (Breastcancer.org, 2022). Also, insulin levels in obese women are higher, another hormone which has been associated with some cancers, especially breast cancer (van den Brandt *et al.*, 2021; CDCBreastCancer 2022).

2.5.9 Chest Exposure/radiation

Women who encounter radiations to the chest area either for diagnosis or treatment for other diseases or cancers at younger ages have a notably higher risk for breast cancer (Moskowitz *et al.*, 2014). This is highly dependent on the woman's age at exposure to the radiation, riskier at teen ages or young adult ages where the breast is yet still developing lowers after 40 years (Yaffe & Mainprize, 2011).

2.5.10 Childbirth

Women who have not been able to keep or complete a pregnancy term or whose first child comes after their 30th birthday tends to be at higher risk of breast cancer (Zhang *et al.*, 2012) compared to women who have had a full pregnancy term before age 30. Significantly, the birth of a child lowers a woman's risk of breast cancer (Eaton, 2002). It is however proven in the literature that the risk of breast cancer increases exponentially in the years just after childhood and this trend, as a result, induces a growth enhancement effect on cells by hormonal variations during pregnancy (Wohlfahrt, 2001).

2.5.11 Breastfeeding

Breastfeeding is largely beneficial to the infant, by reducing many childhood infections (Mother and Child, 2019). Breastfeeding is not just beneficial to the baby but also to the mother by reducing breast cancer risk and other health benefits like reducing the risk of ovarian cancers (Cramer, 2012). Literature linking breastfeeding to breast cancer is expanding. Breastfeeding for at least 12 months is advisable for all women since it is a modifiable risk factor (Breastcancer.org, 2022).

2.5.12 Physical Activities

Being physically active is of great importance to the body. The evidence is increasingly clear that regular physical activity helps to reduce breast cancer risk, mostly after menopause (Breastcancer.org, 2022). This has a massive effect on the body's weight, and hormone levels.

2.5.13 Alcohol

People who are very heavy drinkers, i.e. tend to have improper meals without fruits and vegetables (Breastcancer.org, 2022). Evidence from the literature shows that alcohol increases the risk for

breast cancer (Coronado *et al.*, 2011) and a woman's risk of the disease slightly increases with the increased intake of alcohol since alcohol contains a crucial compound with dire effects. The level of risk is directly proportional to the amount of alcohol the woman drinks relative to women who do not drink any alcohol at all (Breastcancer.org, 2022). Alcohol drinking and tobacco smoking show an interaction in the aetiology of several cancers (ACS, 2022).

2.5.14 Family Related Factors

Amongst all cancers, breast cancer is highly likened to the prevailing family trends, thus breast cancer risk in a particular family is directly proportional to its prevalence in the family (Dumitrescu & Cotarla, 2005). Notwithstanding, the risk of breast cancer for a woman whose close relative such as the mother or sister has had the disease at an old age and without any other family member developing the disease may be comparatively and largely low, whiles a woman is at a higher risk if she has multiple of her family members diagnosed of breast cancer at younger ages (Liu *et al.*, 2021). It is however evident that near one-quarter of the incidence of the disease is related to its existence in the family (Bistoni & Farhadi, 2015).

2.5.15 Environmental Factors

The unavoidable exposure to ionizing radiation, whether through nuclear accidents/explosions or medical, be it for diagnostic/therapeutic purposes, highly increases the risk of breast cancer (Golubicic *et al.*, 2008). The breast is radiosensitive (Mehnati *et al.*, 2019) and the lengthy delay for breast cancers caused by exposure to radiation, in addition to the high response to mutation impairment in developing breasts, after forty years, radiation exposure produces a negligible increase in cancer risk, but on the other hand, early life exposures is a detrimental risk (Ronckers *et al.*, 2004). Supplementary environmental factors, including the vulnerability to electromagnetic

fields and some organochlorine pesticides, are seen to contribute to the increased risk of breast cancer, but more data is needed before drawing firm conclusions.

2.5.16 Genetic Factors

The probability of inheriting breast cancer is partially associated with the gene defect of genes of the breast, like BRCA1 and BRCA2 (Fackenthal & Olopade, 2007). The early identification of these genes (BRCA1 and BRCA2) provides new insights and helps in the prevention of the disease. When the disease is diagnosed at a young age or when multiple relatives are diagnosed with the disease or when there exists enough history of some other cancers in the family, then the woman is exposed to a large risk of breast cancer. Also, when a woman experiences a gene defect in any of the genes (BRCA1 and BRCA2) or when a man experiences gene defects in BRCA2 then they may develop breast cancer with a lifetime risk (Gethins, 2012; Giordano *et al.*, 2002).

2.5.17 Hormonal Factors

Many studies have identified that in most women, the abnormal growth of cells in the breast is related to the reproductive hormones women possess and their continuous exposure to several estrogens (Breastcancer.org, 2022). During pregnancy, the breast cells experience diverse differentiation resulting in a longer period for DNA repair (Albrektsen *et al.*, 1995). Though available data suggest that prolonged lactation reduces the risk of breast cancer, abortion by the use of contraceptives on the other hand has a dire risk of breast cancer, whether spontaneous or induced, escalates the risk of breast cancer (Mørch *et al.*, 2017). The termination of a pregnancy may also terminate/stop several growth changes in the breast and hence increasing the breast cancer possibilities. At this stage, very saturated estrogen levels of early pregnancy are released to and by the breast.

2.5.18 Ductal Carcinoma in Situ (DCIS)

The widespread screening with mammography has improved the detection rate of DCIS significantly (Groen *et al.*, 2017), whiles the breast-conserving therapy's use for the treatment of invasive carcinoma has led to the enhancement of the management of women with DCIS. DCIS is an entity distinct in both its clinical presentation and its biological potential from the other lesion classified as noninvasive carcinoma (Pinder, 2010).

2.5.19 Benign Breast Conditions

Women who have some existing breast conditions are likely to have an increased probability of breast cancer risk (Breastcancer.org, 2022). Often, several of these conditions appear to be more connected to the disease at risk than others. If a woman has a trace of breast cancer and hyperplasia or atypical hyperplasia in her family, she is highly prone to breast cancer (Page *et al.*, 2003).

2.6 Breast Cancer Screening

Though diagnostic mammography and screening mammography differ, they are both used for breast cancer detection. Patients exhibiting symptoms of breast cancer are recommended for diagnostic mammography whiles women without symptoms undergo breast screening (Jatoi, 1999). Screening mammography is purposefully done to find cancers at a so much early stage without it not spreading to other parts to reduce breast cancer mortality by using better treatment options just as the same applies to all kinds of diseases. Mammography has over the years proven efficient amongst other modalities such as clinical breast examination, breast self-examination, screening ultrasonography, magnetic resonance imaging and breast tomosynthesis (ACS, 2022). Mammography screening options are available to all women, especially for women between the ages of 40 and 55, such women can schedule an individual screening plan or may have themselves

screened each year or every other year until they are convinced of a healthy breast (Monticciolo *et al.*, 2017; Oeffinger *et al.*, 2015).

2.7 Mammography

Mammography is a radiographic (X-ray) procedure optimized (low dose) solely for the examination of the breast with the abilities of early breast cancer detection and improving survival rate (Gardner, 2006; Schleede *et al.*, 2014). Whether screen-film or digital, mammography is an effective and widely used examination in medical imaging for the breast with emphasis on low patient motion, high contrast, low noise images, and other important image assessment conditions. Mammograms or mammography is not perfect whether being used as a screening or diagnostic tool, some breast cancers or lesions (micro-classifications) may go unidentified (Dzidzornu *et al.*, 2021). If lesions are detected, further examinations may be conducted to understand their extent. A normal mammogram may consist of either medial-lateral oblique (MLO) or craniocaudal (CC) views. For adequate image quality and maximum clarity in viewing mammograms, correct breast positioning and breast compression are highly important (Meaney *et al.*, 2000). The quality of mammographic images is extremely crucial and essential for the maximum assurance that the entire imaging system of various techniques is working optimally hence the need for regular mammography quality control tests. During a mammography examination, the breast is adequately compressed to evenly spread out the thickness of the breast hence increasing image quality. Compression also, among other things, reduces the thickness of the breast tissue for X-rays to penetrate unperturbed and reduces scatter radiation which hitherto may increase the amount of required radiation dose and reduce image quality (Wikipedia, 2022). Until recently, screen-film systems were largely used in mammography. But for the demands for higher spatial resolution and

other factors, digital mammography or Full-Field Digital Mammography (FFDM) is gradually taking over (Lewin *et al.,* 2002).

2.8 Computed Radiology Digital Mammography

Computed radiology (CR) digital mammography is similar in technology to Full-field digital mammography (FFDM) except for the image receptor. CR employs the photostimulable phosphor (PSP) plates which must be sent to a digital scanner (or reader) and read using a laser beam to extract the stored image to a digital display (Yaffe, 2010). This imaging system also relies on picture archiving and communication systems (PACS) for the transfer and storage of digital images. CR systems also use a PSP plate to store images emerging from the interaction of x-rays with the phosphor. This stored image is then stimulated by a laser beam with a very small focus (Carter & Veale, 2022). This stimulation results in the emission of light which is captured and digitized to produce the digital array. CR is unreliable in terms of image quality for patient dose ranges due to the initial storage, and the stimulation and readout of the image information but highly efficient for high spatial resolution by employing the use of thinner phosphor materials with a finer sampling pitch (Pongnapang, 2005).

2.9 Full-Field Digital Mammography

Over the past twenty years and so, digital mammography has become more relevant than just a simple innovation to becoming the most useful imaging tool for early breast cancer detection (Lewin *et al.,* 2002). Full-Field Digital Radiography (FFDM) is a type of digital mammography that uses x-ray very sensitive plates to rightly gather data during a breast examination and quickly and easily transfers same to a programmed system without using an intermediate cassette (Marchiori, 2004; van den Brandt *et al.,* 2021). The advantages of FFDM

include but are not limited to its time efficiency in processing and the ability to digitally store, transfer and enhance images quickly and easily (Seeram, 2019). Also, less radiation can be used to produce the image's desired quality. Unlike the use of X-ray film, digital radiography employs the use of a digital image capture device. Thus, digital mammography distinguishes the image acquisition process from the substantive display of the image. This is more advantageous by producing immediate image preview and availability, doing away with costly films and processing steps, a very wide dynamic range, with other processing techniques that enhance the overall display of quality images. Flat panel detectors (FPDs) are the most recommended for digital detectors (Neitzel, 2005), these detectors are grouped as direct and indirect FPDs. The indirect FPDs are made up of amorphous silicon (a-Si) is the most readily available material for commercial FPDs. Being combined with a scintillator in the detector's outer layer, also made from Caesium Iodide (CsI). This converts X-rays to light hence the a-Si detector is referred to as an indirect imaging device. The light is channeled through the a-Si photodiode layer where it is converted to a digital output signal. The Direct FPDs on the other hand is made up of amorphous selenium (a-Se) FPDs, and they are also called direct detectors since the X-ray photons are converted directly into charges. The outer layer of the flat panel in this type is a high-voltage electrode. X-ray generates radical electron pairs in a-Se, and the transit of these electrons and holes depends on the potential of the bias voltage charge (Wikipedia, 2022).

2.10 Image Quality and Lesion detectability

The necessity of image quality for accurate and early detection of breast lesions is of utmost importance to every mammography system making it the goal of each piece of equipment used in mammography. Widely, the dependence on high-quality images in mammography makes the modality the most reliable in the accuracy of breast lesion detection. The term 'image quality'

refers to the clarity of images and the ability to present radiologically relevant details in an image. In the context of breast imaging, the ability to detect breast lesions must correspond to the high quality of mammographic images." (Haus & Yaffe, 2000). Screening mammography is an important tool for breast cancer diagnosis and it is frequently used for its early detection (Siu, 2016). Digital mammography provides the potential for a high detection of breast lesions (Pisano *et al.*, 2000), but may be less effective for the detection of small lesions or microcalcifications within dense breasts (Wang, 2017). But for the mammography image to detect early any lesion or microcalcification, the system must exhibit a comparative high contrast since the breast is made up of tissues with almost equal radiation attenuation. Several studies have shown that the cancerous tissues are often denser than the non-infected tissues, hence the amount of X-ray attenuation is expected to be relatively higher, resulting in the contrast variation in the image produced. Digital mammography enables the ability for improved breast lesions detection (Schueller *et al.*, 2008). The higher lesion detectability is directly proportional to higher diagnostic/image quality, and since this is also related directly to an increase in the radiation dose, the radiation delivered must be as low as reasonably achievable (IAEA, 2016). Optimization in mammography systems is so important to image quality and diagnostic accuracy, the best performance of image quality parameters with the radiological dose must be kept as low as possibly achievable, without gaining the best diagnostic outcomes (IAEA, 2016). The Image quality evaluation practice in mammography is an effective support system designed for maintaining high standards, and effective cancer detection and diagnosis (Perry *et al.*, 2008). The Commission further defined the mammographic image quality criteria to include. The image quality criteria defined by the Commission refer to the accurate representation of the internal structures of the breast, and other physical attributes such as contrast, sharpness, artefacts and visualization of microcalcifications. In the image quality assessment, the use of physical quantities such as the measure of contrast,

spatial resolution, noise, modulation transfer function (MTF), detective quantum efficiency (DQE) (Perry *et al.*, 2008) and others. Also, the signal difference to noise ratio and the spatial resolution in the system must show lesion and microcalcifications in the breast, its number and size/shape for appropriate interventions. The lesion detectability increases with a decrease in resolutions (Gagne *et al.*, 2001), thus the lesion detection improves within a certain resolution range whiles microcalcification detection decreases at lower doses with roughly a square root dependence on dose (Gagne *et al.*, 2005).

2.11 Breast Compression

Breast tissue is randomly flexible, comprising more of the fibro-glandular tissues which decrease exponentially with increasing pressure, unlike fat. Breast compression is useful in the reduction of the mobility of the breast, reduction of scattered radiation, spreading of superimposed tissues and also reducing radiation absorbed by glandular tissue in the breast. The only limitation is the worry of some women about the compression pain and the uncomfortable nature of the process scaring many away from undertaking regular screening programs (Dustler *et al.*, 2012). The European Commission outlines several recommendations including the limiting threshold of the compression force not exceeding 200 N. The appropriate compression is a major contributing factor to the quality of mammographic images, enhancing visualization of lesions whiles reducing radiation scatter and breast dose. The aggregate of breast compression during mammography largely contributes to the image quality achieved (Haus *et al.*, 1977).

2.12 Spatial Resolution

Some pertinent details in the breast may be of low-medium contrast and detecting such may not be restricted to high contrast spatial resolution but by contrast resolution. In mammography, the

appropriate description of spatial resolution is the potential of the modality in capturing and recording outstanding spatial details and this is crucial to image quality and breast lesion detection. The need to detect microcalcifications dictates that the spatial resolution should be significantly higher than it is for normal radiography. If the appropriate resolution is not achieved as a result of blurring or breast positioning in the image acquisition and breast motion, image blurring is inevitable where details of the image are spread across structural boundaries (Haus & Yaffe, 2000). The modulated transfer function is considered a more complex mode of measuring resolution through the exhibition of the thin relationship that exists between contrast and resolution in imaging. In the same trajectory, an increase in the spatial resolution increases the visibility of breast details enhancing breast lesion detectability and this knowledge inspired the current design of digital mammography systems with a high spatial resolution (Yaffe, 2010).

2.13 Noise

The major source of distraction for mammographic imaging is the discrepancy in the anatomical background which can confound diagnostic tasks. Noise is a collection of all disordered signals overspread on the relevant signal in the measuring chain or the transmission system (Haus *et al.*, 1977). The useful signal represents the desired details whiles noise is a perturbation in understanding the usable signal, often noise hides or disturbs the clarity of breast details of interest. Anatomical noise which occurs as a result of normal tissue composition in a radiological image has similar energy dependence as the contrast (Izdihar *et al.*, 2015). When anatomical noise dominates, there is a loss in image quality thus preventing the observer/radiologist from seeing the pathological details they are looking for though the anatomical background only partly acts as noise, and the observer is partly able to ignore the anatomical background in the detection task. Breast lesion detection on a mammographic image does not have equal interpretation if it appears

on an adipose or glandular background. Bochud *et al* (1997) proved that anatomical noise contributes tremendously to the system's noise when detecting small spherical objects in mammography (Bochud *et al.,* 1997). Noise levels may be different based on the manufacturer of the system under consideration knowing that the noise in an image increases as the detector pixel size decreases. In digital mammography, there is no usefulness for the film's receptor granularity however, there may be differences in the sensitivity of the receptor, resulting in images unrelated to the detailed tissues in the breast (Fredenberg *et al.,* 2011). As long as the system design ensures that these variations are unperturbed, the noise can largely be eliminated by imaging with uniform X-ray fields and the use of the recorded image as a correction mask to make the image uniform.

2.14 Artefacts

Lesion detection in mammography can be a very difficult task because it must be done in the presence of complex breast structure that is often highly variable over the mammogram and differs from patient to patient. Artefacts or undesired contrasts appearing in the image with unrelated anatomical structures in the breast go a long way to lower the quality of the image or increase noise whiles reducing the detection of lesions or difficulty in the interpretation of images (Li *et al.,* 2010). In digital systems, a component of the image receptor and miscalibration or nonuniformity in the detector feedbacks within the same image perimeter. It is worth noting that can easily be eradicated or reduced when the mammography unit is well designed, maintained and properly calibrated (Yaffe, 2010). Artefacts easily mimic lesions and may distract observers hence the specific artefacts per the system in use must be identified, studied/understood and most importantly avoided to enhance the quality of the image. In digital mammography systems, artefacts are categorized into, hardware artefacts, patient-based artefacts, and technologist and software-based artefacts.

2.15 The Automatic Exposure Control

The automatic exposure control (AEC) system plays an important and basic role in establishing the equilibrium in image quality and the breast absorbed dose in mammography thus achieving a recommendable dose and maximum image quality without the limitations of the composition or thickness of the breast (Salvagnini *et al.,* 2011). In full-field digital mammography (FFDM) systems the AEC form is built to hold pixel value constant even when the thickness or the size of the breast changes and its dependency on contrast does not apply to images captured by the digital detectors but signal-to-noise ratio (SNR). Therefore, most digital mammography AEC modes are built to keep the signal generated by the X-ray detector constant as a function of beam quality (Salvagnini *et al.,* 2015). This however is not a guarantee for improved lesion detectability at different thicknesses. The algorithms behind AEC are keen on the optimization of the X-ray technique (kVp and mAs), the exposure time, and the target/filter combination for a given breast thickness and density. An automated AEC system picks all the necessary exposure parameters, with no operator intervention.

2.16 X-ray Spectrum

Understanding the X-ray energy spectrum from a diagnostic X-ray tube is crucial for effectively ranking its image quality and absorbed dose to the patient. The need to improve mammographic image quality has been ascertained. Although mammography is a widely used modality for the early detection of breast cancer, the system's sensitivity/image quality is largely lowered with breast thickness and density (Izdihar *et al.,* 2015). Factors such as the x-ray spectrum, characterized by the anode/filter combination and tube potential, play a fundamental role in affecting both image quality and absorbed dose whiles image contrast was been shown to be independent of selected mAs values/radiation intensity (Huda *et al.,* 2003). When both the X-ray tube output mAs and X-

ray tube voltage kVp are selectively diversified, there appears corresponding variations in image quality and dose with references to the existing tradeoffs between dose and image quality in digital mammography for the detection of lesions within an average breast. Changes in the mAs value affect just the beam quantity and without an effect on beam quality whiles the doses increase with a rise in kVp since both beam quality (more penetrating radiation) and quantity (higher tube output) increase when the kilovoltage setting is increasing (Dance *et al.*, 2000). The use of digital mammography imaging systems strives to keep patient doses as low as reasonably achievable hence a relatively low photon energies spectrum is used to produce the high contrast sensitivity, this energy spectrum can be altered to meet prevailing breast sizes whiles appropriating contrast and radiation dose to the breast. The merger of a molybdenum anode and a molybdenum filter (Mo/Mo) has over the period been the preferred choice for mammographic X-ray tubes. However, there are systems with different anode/filter combinations such as molybdenum/rhodium (Mo/Rh), rhodium/rhodium (Rh/Rh), rhodium/aluminum (Rh/Al) and tungsten/rhodium (W/Rh) are now in use largely (Huda *et al.*, 2003). These new X-ray spectra produce different and improved imaging and dosimetry performance.

2.17 Signal-to-Noise Ratio (SNR)

To measure the detection rate of an object such as microcalcifications/lesions in an image, the signal-to-noise ratio (SNR) is largely applicable. The signal-to-noise ratio is a generic measure of the actual signal that reflects the true anatomy of noise or a measure of the image signal in a given region (ROI) to the background (Bochud *et al.*, 1997). A lower signal-to-noise ratio generally results in a grainy appearance of images, hence a dependent parameter to measure the ability to visualize objects in a noisy background. Using the Albert Rose's model, which is a measure of the image signal in a given region is compared to the background of the mammography image (Erwin

et al., 1996). Albert Rose's model is a mathematical model that describes the perception of contrast in an image. It is used to evaluate the quality of mammography images. Since photon noise is considered to be the dominant source of noise, any increase in the number of photons, such as increasing the mAs (tube current-exposure time product), increases the signal-to-noise ratio (Lemacks *et al.*, 2002). Also, as shown by Nishikawa & Yaffe (1985), the signal-to-noise ratio (SNR) is associated and similar for systems at low frequencies, while at higher frequencies, SNR is determined by the modulation transfer function (MTF). The systems having higher MTF have higher SNR. The MTF is a measure of the ability of an imaging system to transfer contrast from the object to the image. A higher MTF indicates that an imaging system can better distinguish between different parts of an object. The diagnosis of breast cancer from a mammographic image requires the visualization of normal breast anatomy and soft tissue pathology as well as lesions which can be almost negligible in diameter. The ultimate limit of detection of subtle lesions in a radiological image depends not only on signal and contrast but also on SNR. SNR-dependent parameters are noise-equivalent quanta (NEQ) and the detective quantum efficiency (DQE) (Lemacks *et al.*, 2002).

CHAPTER THREE

MATERIALS AND METHODS

3.1 Overview

This chapter gives detailed description of materials and methods used in gathering and analyzing collected data during this study. This chapter also provides the step-by-step procedures used to achieve the expected results.

3.2 Materials

Materials utilized during the study involved the mammography machine, the American College of Radiology mammography accreditation phantom, (ACR MAP), semi-circle polymethylmethacrylate (PMMA) slabs, Digital Imaging and Communication in Medicine (DICOM) software, Piranha Quality Control kit, Ocean 2014 software, ImageJ software, bathroom scale, towel, lawn tennis ball, a meter rule, aluminum filters, and Microsoft Excel 2010 software.

3.2.1 Mammography Machine

Five digital mammography machines installed at five different facilities (3 hospitals and 2 diagnostic centers) were used for this study. The facilities were the University of Ghana Medical Centre (UGMC), Korle - Bu Teaching Hospital (KBTH), 37 Military Hospital, the Diagnostic Centre and the Paradise Diagnostic Centre. All the three hospitals are government owned whiles the two diagnostic centers are private owned. As at the time of this study, the mammography equipment at KBTH and 37 military hospital were FFDM whiles the other three (3) facilities were CRDM. Specifications of the mammography machines are summarized in Table 3.1 and Figure 3.1 shows the image of a typical mammography machine.

Table 3.1: Specifications of the mammography machines used for this study

SPECIFICATIONS	SYSTEM A	SYSTEM B	SYSTEM C	SYSTEM D	SYSTEM E
Equipment Type	FFDM	FFDM	CRDM	CRDM	CRDM
Manufacturer	Helianthus	Siemens	Philips	Varian Medical systems	Planmed OY
Equipment Model	Helianthus C	Mammomat Inspiration	MammoDiagnost AR	Alpha RT	Nuance
Manufacture Year	2019	2018	2015	2013	2009
Serial Number	M845W/67 W189	(422)276/(21)11076	MAR/0036/CSO	16370	SMH 40967
Function Mode	AEC/Manual	AEC/Manual	AEC/Manual	AEC only	AEC/Manual
Anode/Filter Type	W/Rh	W/Rh	Mo/Rh	Mo/Rh	Mo/Mo
SID (mm)	65cm	65cm	65cm	60cm	65cm
kVp Range	20-35	20-35	20-35	22-30	20-35
mAs Range	1-640	1-600	1-640	40-120	10-400

Figure 3.1 Image of a Mammography machine (Field Work)

3.2.2 Polymethylmethacrylate (PMMA) Slabs

Poly (methyl methacrylate) is the scientifically approved name for the synthetic (resin) polymer commonly referred to as acrylic glass. The PMMA shown in Figure 3.2 is a thermoplastic which appears transparent in nature, it is highly compatible with the human tissue hence its use in the production of lenses which are implanted in the human eye for the correction of cataracts. Phantom-based studies and measurements in radiology especially mammography uses the PMMA for Quality Control (QC) test including the various step by step approaches of evaluating optimum functioning of the X-ray machines. The Polymethyl Methacrylate (PMMA) is one of the most appropriate media for breast modeling. The PMMA slabs used in this study were in 10 mm and 5 mm respectively but paired as 20 mm, 45 mm and 70 mm.

Figure 3.2. Image of the PMMA slab (Field Work)

3.2.3 The TORMAS Phantom

The TORMAS phantom is a Leeds testing tool primarily utilized for the mammography image quality test under quality control. It is thought to be the UK's most sensitive test object and is made to be used quickly and easily on a regular basis to provide equipment effectiveness checks of imaging performance. The TORMAS phantom's internal features allow for the verification of a ten-step grey-scale wedge, a high-contrast resolution limit (1.0 to 20.0 lp/mm), low-contrast large-detail detectability (12 details, 5.6 mm diameter), high-contrast small-detail detectability (11 details, 0.5 and 0.25 mm diameter), irregularly shaped particles on a step-wedge background (median sizes 125, 234). Figure 3.3 shows the TORMAS phantom used in the study with serial number 443.

Figure 3.3: The TORMAS Phantom (Field Work)

3.2.4 American College of Radiology Mammography Accreditation Phantom (ACR MAP)

The American College of Radiology Mammography Accreditation Phantom as shown in Figure 3.4 is an acrylic phantom purposefully used for verifying the performance of a mammography unit using the visualization abilities to qualitatively evaluate a unit's capability to capture tiny masses comparable to relevant microcalcification for early detection breast cancer detection. The phantom's objects resemble tumor masses, fibrous microcalcifications and calcifications. The ACR MAP consists of a wax block embedded with six nylon fibers varying in thickness through 0.40 mm towards 1.56 mm, five (5) groups of six high contrast simulation microcalcifications/specks, each with an individual diameter of 0.16 mm to 0.54 mm, and five groups of five low contrast simulation masses, each with an individual diameter of 0.25 mm to 2.00 mm, for a total of sixteen different test objects (ACR, 2019). The ACR MAP simulates a flatten breast tissue like 4.2 cm average glandular/adipose constitution, 50 % of adipose tissue and 50 % of glandular tissue. It also provides physical standard baseline which assures quality images and tests systems sensitivity and quickly detects objects from 0.16 mm to 2.0 mm. The ACR MAP phantom used in this study is manufactured by Gammex with serial number 800004-1410115.

Figure 3.4: The American College of Radiologist Mammography Accreditation Phantom (ACR MAP) - (Field Work)

3.2.5 Digital Imaging and Communications in Medicine (DICOM)

The National Electrical Manufacturers Association (NEMA) created the Digital Imaging and Communications in Medicine (DICOM) protocol in the early 1990s. It is now a widely used transmission tool for medical imaging and the file format of images obtained from different imaging methods in medicine, including computed tomography (CT), mammography, magnetic resonance imaging (MRI), ultrasound imaging, and radiography, among others. (DICOM, 2012). It has been widely adopted in medical facilities that use medical imaging, and as more hospitals, clinics, and practices start to digitize their medical imaging, archiving, and distribution processes, its application is growing to include many other medical specialties besides radiology. The DICOM software was used in this study to efficiently integrate imaging devices, servers, workstations, printers, and PACS (Picture Archiving and Communication System) from various

manufacturers, enabling the archiving, retrieval, and distribution of phantom images and related information as well as ensuring interoperability between medical imaging computer systems. For additional analysis, the DICOM files were exported or saved in other formats like the JPEG format.

3.2.6 Piranha Multimeter

Piranha is a Radiation to Information (RTI) package used for an instant X – ray quality control and quality assurance solutions. It is an all-in-one multimeter that can be connected to a computer remotely or via Universal Serial Bus (USB). It works with the diagnostic RTI software ocean 2014, which is used to display, record and report all the measurements, waveforms and facilitate the reading on a screen. For radiography, fluoroscopy, CT, dental, and mammography, use a Piranha QC multimeter. It instantly and simultaneously measures and displays all parameters. The Piranha meter is used in the company with the Ocean 2014 software to display parameters such the tube voltage (kVp), exposure time, half value layer (HVL), total filtration, Dose, Dose rate and presents waveforms. The Piranha system used in this study is the Piranha 657, version 5.5 with serial number, CB2-15020088. Figure 3.5 shows the Piranha QC meter used for this study.

Figure 3.5: The Piranha multimeter (Field Work)

3.2.7 Ocean 2014 Software

Ocean 2014 is a powerful tool for everybody working with Quality Assurance of X-ray systems (Ocean 2014, 2015), whose interface is shown in Figure 3.6. It is the preferred diagnostic software used with radiation-to-information (RTI) instrument. On a simple-to-read screen, it shows all measurements and waveforms gathered. The Piranha QC meter if plucked to a computer which has the ocean 2014 software already installed on it makes the special quick check runs automatically upon detecting the Piranha QC meter. Gathered data can easily be migrated to Microsoft Excel, printed or saved manually. The software enables a carefully thought-out measurement protocol which can eliminate any setup uncertainties. As a result, there will be fewer

errors, more efficiency, and better workflow coordination. Users within the same facility can easily share their measurements and templates with coworkers.

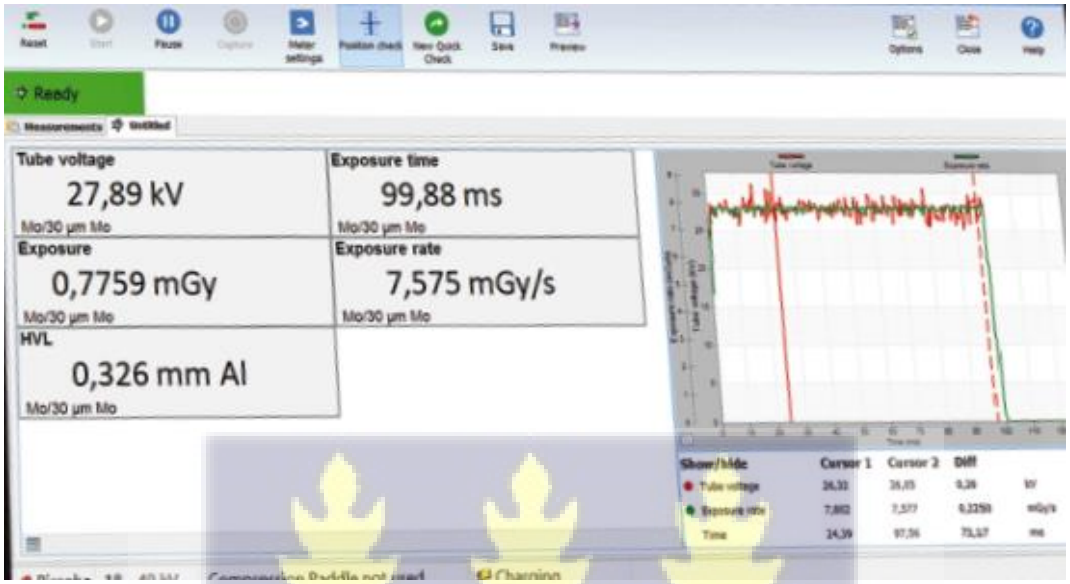

Figure 3.6: Interface of the Ocean 2014 software (Field Work)

3.2.8 Microsoft Excel 2016

The software used for the data analysis in this study was Microsoft Excel 2016 version 14.0 included in Microsoft office 2016 installed on a Windows 10 system. Microsoft Excel which is a spreadsheet developed for Windows functions by solving statistical, engineering and financial problems and it is used to display data as line graphs, histograms and charts. It supplies pivot tables and scenario manager that can be used to section data in order to view dependencies between variables (Greg, 2007). It can also be used for numerical methods to solve differential equations in mathematics and physics. Excel 2016 was used to prepare the main data collection sheet for this study and to perform some of the analyses. Figure 3.7 shows the interface of excel 2016 running on Windows 10.

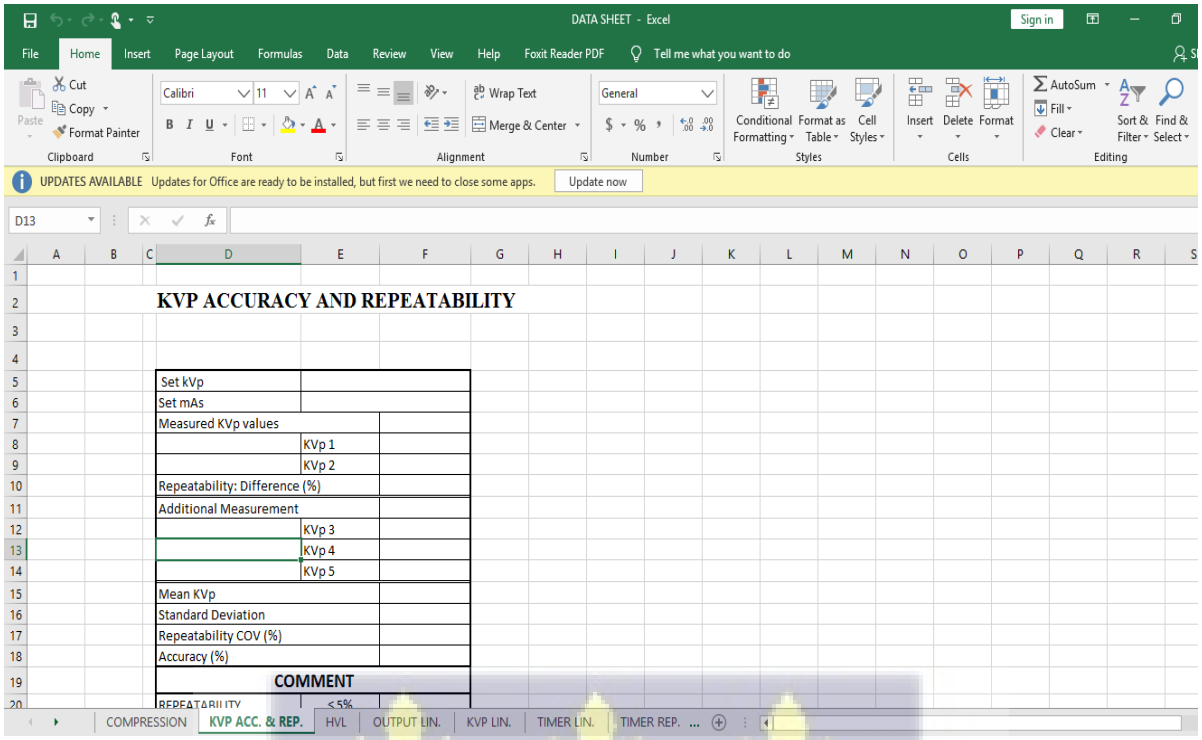

Figure 3.7: Interface of Microsoft Excel 2016 (Field Work)

3.2.9 ImageJ Software

ImageJ is a potent image analysis program (LOCI, University of Wisconsin). It is a free Java image processing program that can be downloaded or used online on any computer with a Java virtual machine version 1.1 (ImageJ Manual, 2022). 8-bit and grayscale, 16-bit, and 32-bit images can be displayed, edited, examined, processed, saved, and printed using ImageJ. The software whose interface is shown in Figure 3.8, is able to read text-based unprocessed files, like data from spreadsheets, as well as other image formats, including TIFF, GIF, DICOM, FITS, and JPEG. It can measure distances and angles as well as compute statistics for the area and pixel values of specific regions. Measured values can be quickly and easily "cut and pasted" into a spreadsheet during analysis. The open architecture of ImageJ makes it possible for users to create plugins that solve a variety of image processing and exploration issues, including automated hematology

systems, rounded live-cell imaging, radiological image processing, and large imaging unit information collations.

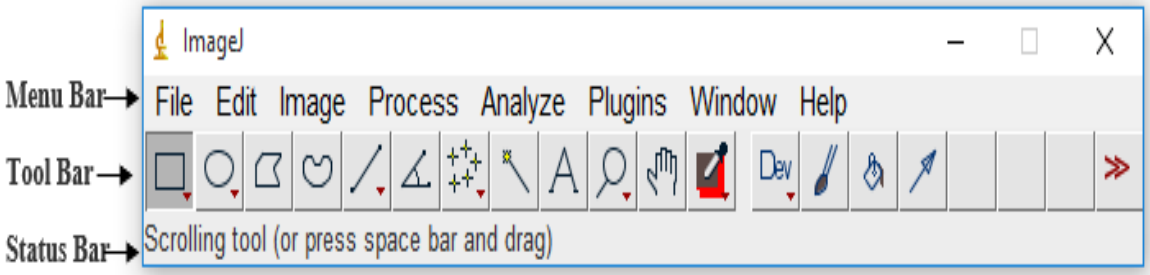

Figure 3.8: The interface of the ImageJ software (Field Work)

Additionally, ImageJ supports common image processing operations like edge detection, sharpening, smoothing, convolution, Fourier analysis, and median filtering. It also supports contrast manipulation and Fourier analysis. It performs geometric transformations like flips, rotations, and scaling.

3.3 Methodology

Quality control (QC) also referred to in this study as the pre-exposure/exposure test is a very essential aspect of quality assurance (QA) which involves frequent and annual assessment of the components of an imaging system. Some QCs were performed on the mammography equipment used in this study to ensure their optimum performance. Effective quality control (QC) routines have a great impact on improving image quality and reducing dose to the patient. The quality control (QC) examinations performed on all five machines used included compression force, compression thickness, compression alignment, tube voltage (kVp) accuracy and repeatability, output linearity and repeatability, tube voltage (kVp) and time linearity, half value layer (HVL),

and timer repeatability. Quantitative image quality assessments were carried out and the lesion detectability evaluated using observer detection abilities whiles qualitative assessment was done using ImageJ and signal-to-noise ratio calculations. Relevant data collection sheet was designed for recording relevant information from the specific QCs performed. Images acquired from exposures for QC and image quality purposes were exported to the DICOM for further analysis. All the tests were conducted using the IAEA protocols (IAEA, 2009, 2011).

3.3.1 Compression Test

For the purposes of high image quality and maximum reduction in dose, it is highly essential for the mammography system to be adequately compressed. Hence the main rationale of this test was to check whether or not the machine gives sufficient compression, as well as to verify the precision of the compression force (IAEA, 2011).

3.3.2 Compression Force

The bathroom scale was positioned on the platform above a bath towel on the breast support plate. Centrally positioned beneath the compression paddle was the bathroom scale. On the bathroom scale, a lawn tennis was placed to shield the compression plate in the manner that readings on the scale are not disrupted. The indicator reading on the bathroom scales was also adjusted to the zero mark before the activation of compression. The compression plate was released downward by using the manual compression mode and the compression paddle gradually to firmly hold the PMMA slab. As the lawn tennis deflects its reading translated to the bathroom scale is recorded in kilograms (kg) whiles the compression force indicated on the mammography machines was also recorded in Newtons (N), both on the data collection sheet for further analysis. The compression

plate was released using the compression paddle. Tolerance value for the displayed and measured forces should be ±20 N. Figure 3.9 shows the setup for the compression force.

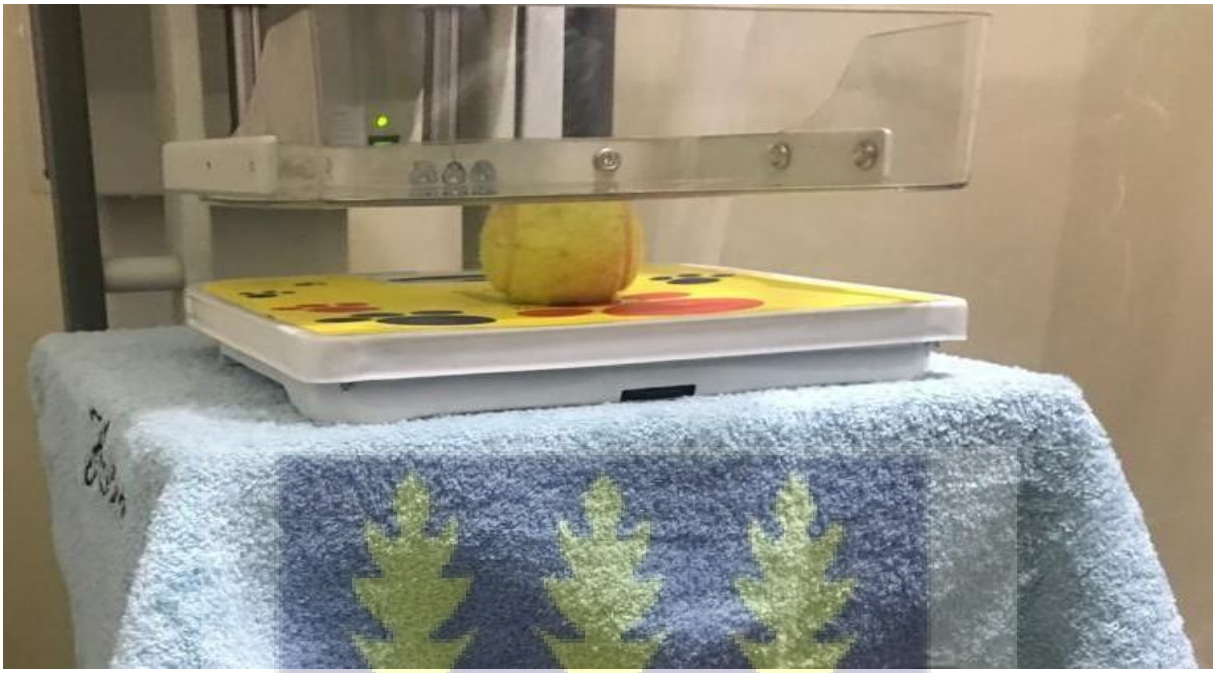

Figure 3.9: Set-up for compression force (Field Work)

3.3.3 Compression Thickness

To stop the compression plate from deforming and lessen measurement errors in the thickness indication caused by the compression plate's tilt angle, an 18 cm × 24 cm PMMA slabs were used. The PMMA slabs of varying thicknesses (20 mm, 45 mm and 70 mm) respectively were in line with the breast support platform's edge along the chest wall. Compression was activated and released gradually until it was firm to the PMMA slabs with regards to the compression force used in the clinical setting, special care was taken not to compress too much. The displayed and the centrally measured thicknesses were recorded on the data sheet and compared, the tolerance limit

of these thicknesses is ± 5 mm of phantom thickness. Figure 3.10 shows the set-up of compression thickness.

Figure 3.10: Set-up for compression thickness and alignment (Field Work)

3.3.4 Compression Alignment

As in the compression thickness test, the PMMA slabs of varying thicknesses (20 mm, 45 mm and 70 mm) respectively were in line with the breast support platform's edge along the chest wall. Compression was activated and released gradually until it was firm to the PMMA slabs with regards to the compression force used in the clinical setting. Special care was taken not to compress too much. The measured thickness was compared to the slab's actual thickness. Additionally, measured and noted on the data sheet was the distance between the compression plate's four corners and the breast support. The minimal misalignment tolerance at both sides (left and right) of the platform should be within ± 5 mm. Figure 3.10 shows the set-up of compression alignment.

3.3.5 Accuracy and Repeatability of Tube Voltage (kVp)

This test's primary objective was to examine the tube voltage's (kVp) precision and repeatability. A nominal tube voltage (kVp) setting of 28 kVp with a set mAs of 50 mAs was used. The Piranha detector was placed on the breast support platform centered laterally and 40 mm from the chest wall. After the necessary alignment and compression, five (5) exposures at 28 kVp and 50 mAs. The Piranha kVp readings were recorded on the data sheet. Excel was used to determine the mean and the standard deviation of the measured kVp values recorded. Figure 3.11 shows the set-up for the kVp accuracy and repeatability.

For the accuracy of kVp, the percent difference between the measured value and the nominal kVp value was determined in accordance with Equation 3.1;

$$Deviation\ (\%) = \left[\frac{kVp_{nom.} - kVp_{meas.}}{kVp_{nom.}}\right] \times 100 \quad \ldots\ldots\ldots\ldots\ldots\ldots\ldots \quad 3.1$$

where kVp(nom) is the value indicated on the equipment and kVp (measured) is the measured value. This percentage deviation is considered the measure of the accuracy which must be within an acceptable $\pm$ 5 % range (IAEA, 2011).

For the repeatability of kVp, the measurement percentage difference was calculated using Equation 3.2;

$$Difference\ (\%) = \left[\frac{Max. - Min.}{Min.}\right] \quad \ldots\ldots\ldots\ldots\ldots\ldots\ldots\ldots\ldots\ldots\ldots\ldots\ldots \quad 3.2$$

Where "Max" denotes the highest measurement and "Min" denotes the lowest measurement. For consistency in kVp, the tolerance limit of the percentage difference ought to fall within the acceptable range of $\leq$ 5 % (IAEA, 2011).

The tube voltage's Coefficient of Variation (COV) was also determined by the Equation 3.3;

$$COV(\%) = \frac{SD}{Mean} \times 100 \quad \ldots\ldots\ldots\ldots\ldots\ldots\ldots\ldots\ldots\ldots\ldots\ldots\ldots\ldots\ldots\ldots\ldots\ldots 3.3$$

Where Mean is the average of the measured kVp values and SD is the measurement's standard deviation. For repeatability, the tolerance of COV (%) should be within the range ≤ 2 % (IAEA, 2011).

Figure 3.11: Set-up for the kVp Accuracy and Repeatability (Field work)

3.3.6 Output Linearity and Repeatability and Timer Repeatability

This test was performed to assess the linearity and repeatability of the exposures for a specific mAs. The detector was placed on the breast support laterally centered 40 millimeters away from the chest wall, for maximum irradiation of the sensitive volume of the detector. The tube voltage

was kept constant at 28 kVp whiles three mAs values were selected between ranges that are used clinically thus 40 mAs, 80 mAs and 120 mAs. At a fixed mAs of 40 mAs, five exposures made whiles two exposure were made for 80 mAs and 120 mAs respectively. The exposure with each time readings on the detector was recorded on the data collection sheet and the percentage difference was calculate for both exposure and measured time using Equation 3.2. Also, the coefficient of variation was estimated for both using Equation 3.3 whiles the mean/average of the exposures at each respective mAs were determined using Microsoft Excel. The set-up for the output linearity and repeatability measurement is the same as the set-up for the kVp Accuracy and Repeatability in Figure 3.11.

By dividing each average exposure value by the corresponding mAs, the output, Y, was calculated, and the results were recorded. By taking two output values (Y_1 and Y_2), the linearity at successive mAs settings (L) was calculate using Equation 3.4 and the result recorded on the data sheet.

$$Linearity\ (L) = \frac{(Y_1 - Y_2)}{(Y_1 + Y_2)} \times 100 \quad \text{..... 3.4}$$

The acceptable tolerance limit; repeatability – difference is ≤ 5 % or coefficient of variation (COV) is ≤ 5 % whiles linearity should be < 10 % (IAEA, 2009).

3.3.7 Tube Voltage (kVp) and Time Linearity

This test was purposefully performed to assess the linear responses of the peak voltage and timer across a range of nominal values while using the same set-up as in Figure 3.11. For the tube voltage (kVp) linearity test, five exposures were made with a fixed mAs of 50 mAs whiles a range on kVp values used, from 22 kVp to 30 kVp with 2 kVp intervals. The exposure readings were recorded

on the data collection sheet for further analysis. A graph of exposure (*mGy*) against kVp^2 was plotted and a line of best fit as well as the R2 value from the were determined. In the test for the time linearity, the respective range of kVp values used in the kVp linearity test was maintained whiles varying the mAs values for each respective kVp. A graph of exposure time (*ms*) against kVp^2 was plotted and a line of best fit as well as the R^2 value from the fit were determined to ascertain linearity of kVp and the time.

3.3.8 Half Value Layer (HVL)

The goal of this test was to establish the HVL and assess whether the X-ray beam's total filtration satisfies the minimal requirements of national and international standards. Exposure parameters used clinically were selected such that kVp was 28 kVp and the detector was placed laterally centered on the breast support platform at 40 mm away from the chest wall, allowing the chamber's sensitive volume of the detector is totally segmented within the radiation field. The compression paddle was also placed approximately halfway between the focus and the detector. After the necessary compression, an exposure was made and readings recorded on the collection sheet. A 0.106 mm of aluminum was placed on the compression paddle totally covering the active volume of the chamber and an exposure was made with the same parameters and recorded. Checks were made to see if the reading is higher than half of the reading without the aluminum, if it is, more of the 0.106 mm thickness of aluminum was add onto the earlier until the half or below half of the exposure value without an aluminum filter was achieved. All the Al filters were removed and the exposure was repeated and readings noted. Exposure values were recorded in the data collection alongside the respective thickness of aluminum used. The half value layer (HVL) was calculated using Equation 3.5;

$$HVL = \frac{t_2 In\left[{}^{2M_1}/_{M_0}\right] - t_1 In\left[{}^{2M_2}/_{M_0}\right]}{In\left[{}^{M_1}/_{M_2}\right]} \quad \text{..... 3.5}$$

Where M_1 and M_2 are the average (mean) values of the readings measured in with the aluminum, and M_0 is the average value of the reading measured without the aluminum, and t_1 and t_2 are the thicknesses (in mm) of the aluminum used. This calculated value of the HVL was recorded in the data sheet. The calculated HVL is acceptable when it falls within the tolerance range in Equation 3.6;

$$\frac{kV}{100} + 0.03 \leq HVL \leq \frac{kV}{100} + C \quad \text{..... 3.6}$$

Where: C = 0.12 for Mo/Mo, 0.19 for Mo/Rh, 0.22 for Rh/Rh, 0.30 for W/Rh and kVp is the measured value for the nominal kVp selected (IAEA, 2011).

3.3.9 Qualitative Image Quality Tests (ACR MAP)

The image quality in mammography has an unwavering important concern in the early breast cancer detection hence the importance of image quality does not change. The ACR MAP has been taken as the most appropriate example (Dance *et al.*, 2000) mimicking a 4.2 cm compressed breast thickness containing object as Six fibers, each with a diameter of 1.56 mm, 1.12 mm, 0.89 mm, 0.75 mm, 0.54 mm, and 0.40 mm, five groups of simulated microcalcifications, each with a diameter of 0.54 mm, 0.40 mm, 0.32 mm, 0.24 mm, and 0.16 mm, and five masses (with thicknesses of 2.0 mm, 1.0 mm, 0.75 mm, 0.5 mm and 0.25 mm). To ensure that the overall image quality has not decreased from baseline performance levels, the image quality test was carried out

in order to establish a baseline level of subjective image quality. The phantom (ACR MAP) was placed on the breast support and centered laterally so that the image receptor's side of the chest wall and the phantom's edge of the chest wall are parallel. The compression paddle was lowered so that it just touches the top of the phantom. Figure 3.12 shows the ACR-MAP set up. Exposure was made using the appropriate exposure parameters/technical factors clinically applicable including the target filter combination for a 4.2 cm thick breast and also in the automatic mode. The exposures were repeated for varying mAs and kVp values such that four exposures were made and achieved images were exported to DICOM for further analysis and the corresponding data was recorded on the collection sheet with the exposure factors and technique used. The number of test objects were counted and scored in each group. Artifacts values were subtracted from the score of the group the artifact falls.

The acceptable tolerance for image quality with the respective objects is as follows (IAEA, 2009):

- ✓ Fibers should be ≥ 4: (completely visual = 1; visual only in part, with more than half - fiber = 0.5 whiles that which is not up a half-fiber = 0)
- ✓ Microcalcifications should be ≥ 3: (groups with four or more visible microcalcifications = 1; the score of 0.5 where 2 to 3 microcalcifications are visible whiles groups where there are fewer than two visible microcalcifications = 0)
- ✓ Masses should be ≥ 3: (totally visualized = 1 whiles partially visualized = 0.5)

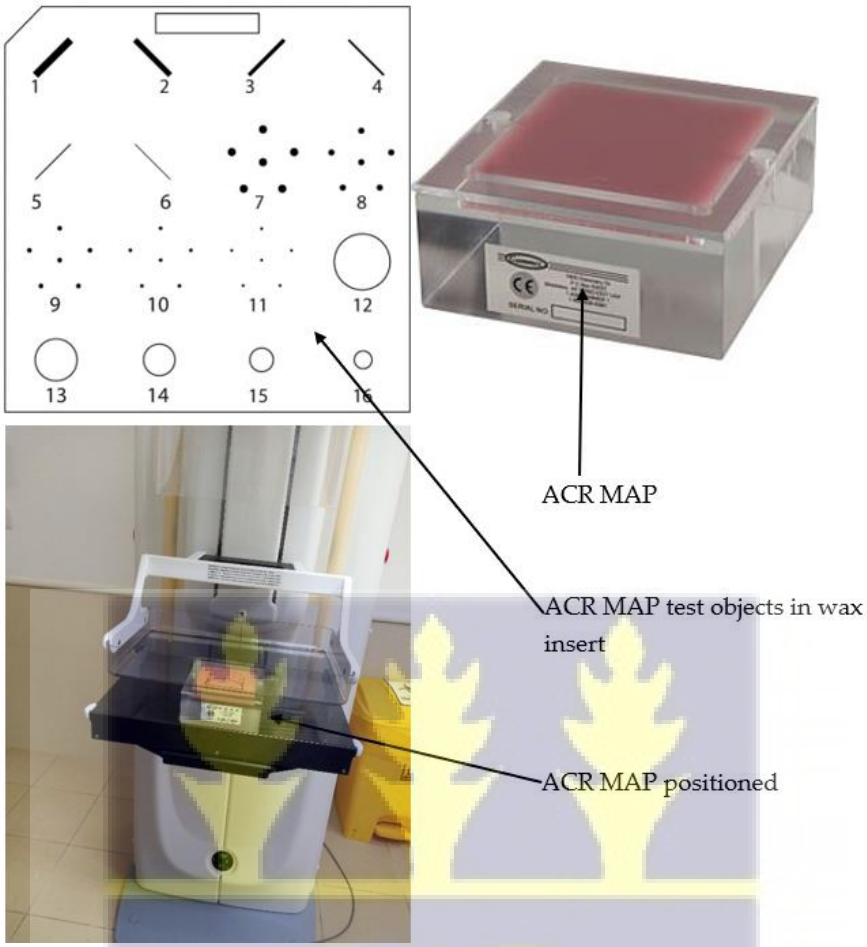

Figure 3.12: Image quality set-up with the ACR MAP (Field Work)

After the respective scoring of the fibers, specks and masses, the visible rates for respective technique factors were to compare the visibility amongst the system. Equations 3.7 and 3.8 were used to calculate the visible rates and the percentage visibilities respectively.

$$Visible\ rate = \frac{mean\ of\ visible\ inserts}{total\ number\ of\ inserts\ in\ phantom} \quad \text{…….. (3.7)}$$

$$Visible\ rate = \frac{mean\ of\ visible\ inserts}{total\ number\ of\ inserts\ in\ phantom} \times 100 \quad \text{……..(3.8)}$$

3.3.10 Quantitative Image Quality Tests (PMMA and Aluminum Filter)

This test is performed with equal relevance as the image quality test using the ACR MAP but with the main intent to determine the signal-to-noise ratio in the imaging system. The PMMA phantom of 45 mm was sandwiched with an aluminum filter in the center and placed on the breast support platform, 5 cm from the chest wall edge whiles centered laterally. Compression was applied and using clinically applicable technical factors for a 45 mm (phantom thickness) compressed breast, exposures was made in the automatic mode was used (AEC was in use). The exposures were repeated for varying mAs and kVp values such that four (4) exposures were made and achieved images was processed as a DICOM image and imported to ImageJ where regions of interest (ROIs) were drawn. A total of five (5 ROIs) were drawn, one ROI in the aluminum and four in the background besides the four corners of aluminum filter in the image. The area, mean and standard deviation in the ROIs were measured and used to calculate the signal-to-noise ratio (SNR) using Equations 3.9 and 3.10 respectively.

$$SNR_{Rose} = \frac{A(\overline{q_b} - \overline{q_o})}{\sqrt{A\overline{q_b}}} \quad \text{..... 3.9}$$

$$SNR_{Rose} = C\sqrt{A\overline{q_b}} \quad \text{..... 3.10}$$

Where $C = \frac{\overline{q_b} - \overline{q_o}}{\overline{q_b}}$ is the contrast, A is the object area, $\overline{q_b}$ is the average quanta per unit area in the uniform background in which the object is and $\overline{q_o}$ is the average per unit area in the region of the object. The acceptable tolerance SNR value should be > 5 (IAEA, 2009) implying that the machine's SNR is good. Figure 3.13 shows the set-up for the PMMA and the sandwiched aluminum filter.

Figure 3.13: Set-up of the PMMA and the sandwiched aluminum filter (Field Work)

3.3.11 Spatial Resolution Test

The aim of this test was to determine the system's high contrast resolution to see if the mammography system can detect two micro-calcifications separately. A mammography Leeds object (TORMAS phantom) was positioned on the Bucky aligned with the chest wall and laterally centered on 40 mm of PMMA shown in Figure 3.14.

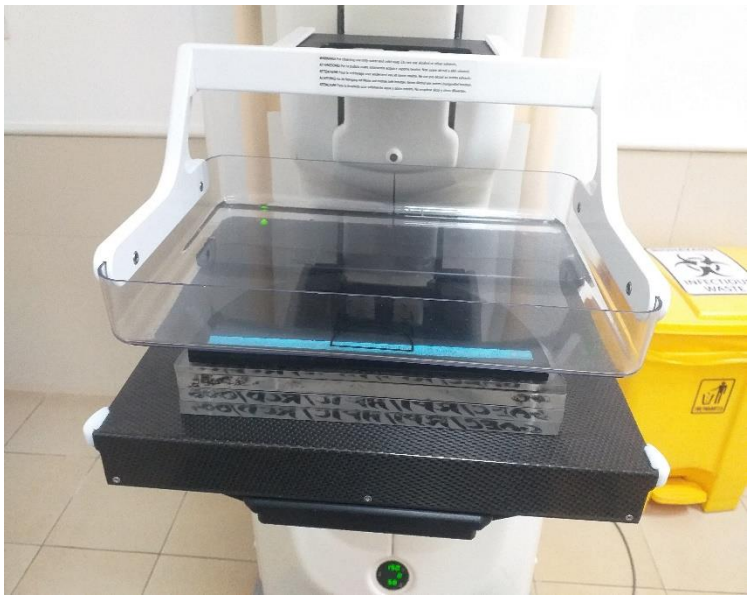

Figure 3.14: Set – up for spatial resolution with TORMAS phantom (Field Work)

The Bucky was loaded with a cassette, and compression was then applied. A 45 mm compressed phantom was exposed using the technical parameters (kVp, grid, filter, and target) that are used in clinical practice (equivalent thickness to 40 mm of PMMA), with varying mAs and kVp. According to the IAEA's HHS numbers 2 and 17 (IAEA, 2009, 2011), the achievable tolerance should be ≥15 lp/mm in both directions whiles the acceptable tolerance should be ≥11 lp/mm in both directions. The image was given a subjective evaluation, and the corresponding information was recorded in the data collection sheet.

CHAPTER FOUR

RESULTS AND DISCUSSIONS

4.1 Overview

The presentation, analysis and discussion of the various test results are presented in this chapter. Discussion is presented about the compression force, compression thickness, compression alignment, tube voltage (kVp) accuracy and repeatability, output linearity and repeatability, tube voltage (kVp) and time linearity, half value layer (HVL), and timer repeatability. Also, image quality results are discussed regarding the ACR phantom and the TORMAS phantom alongside the system's signal-to-noise ratio (SNR) and lesion detection capabilities of the mammography systems. All tests were conducted following recommendations by the IAEA's Human Health Series Numbers 2 and 17 (IAEA, 2009, 2011). The two FFDM systems used in this study are represented by the letters A and B, whiles the CRDM systems are represented by letters C, D and E respectively.

4.2 Pre – Exposure/Exposure Performance Tests

4.2.1 Compression Tests

Inflexible breast compression in mammography amongst other relevant benefits reduces breast motion, reduces breast tissue thickness, and minimizes scatter radiation dose to the breast tissues whiles enhancing the image contrast and maximizing the visibility of microcalcifications. The compression test was performed to verify that the respective mammography systems exert the appropriate and enough compression to conform with the precision in performance relative to the displayed system compression parameters. Regarding the relevant International Atomic Energy

Agency's protocols, the results of all the compression tests showed that the compression paddles of the mammography systems were functioning effectively.

4.2.2 Compression Thickness Test

The compression thickness test was performed on all five mammography systems used for this study and their respective results are presented in Table 4.1. The ± 5 mm tolerance limit of phantom thickness was used as a reference to justify whether or not a system has passed the compression thickness test. Although all the systems passed the compression thickness, systems D and E which also are CRDM systems provided excellent compact compression for the 20 mm phantom thickness. The FFDM systems A and B also provided excellent firm compression for the 45 mm phantom thickness while system A of the FFDM systems and the CRDM's system E provided excellent hardened compression for the 70 mm phantom thickness all showing no difference in the known thickness and the measured thicknesses respectively. It is hence deductive to state that, all the systems used in this study are capable of attaining the needed image quality whiles enhancing the detectability of lesions. The data in Table 4.1 is derived from Appendix C.

Table 4.1: Results of the compression thickness test for all five (5) systems

Mammography Systems	**Compression thickness (± 5 mm)**			**Remarks Pass/Fail**
	20 mm	**45 mm**	**70 mm**	
A	-1	-2	-1	Pass
B	-2	3	3	Pass
C	-2	-2	-1	Pass
D	-1	-2	-1	Pass
E	-4	-1	-2	Pass

4.2.3 Compression Alignment Test

The separation of overlapping breast tissue for maximum X-ray penetration, which simultaneously produces better quality images of the breast tissue whiles decreasing the radiation exposure to patients in need of mammography services is of great relevance. Though achieving the needed compression may be uneasy due to the uncomfortable positioning and compression, it can help improve the image quality. The highest possible results of the compression alignment test from the five (5) mammography systems used are shown in Table 4.2. The values of all the systems both FFDM and CRDM were below the recommended tolerance limit of ≤ 5 mm stated in the IAEA's Human Health Series for digital mammography. This implies that the compression plate in all the systems used in this study is well aligned hence firm and adequate compression is assured for optimal image quality in the various facilities. The data for this test is derived from Appendix E.

Table 4.2: Results of the compression alignment test for all five (5) systems

Mammography Systems	Compression Alignment (≤ 5 mm)			Remarks
	20 mm	45 mm	70 mm	Pass/Fail
A	0	1	1	Pass
B	1	1	1	Pass
C	2	1	0	Pass
D	0	2	1	Pass
E	1	0	1	Pass

4.2.4 Compression Force Test

Results obtained from the compression force test are presented in Table 4.3 whiles the raw data for the same test is presented in Appendix D. Although the systems C and D exhibited higher compression difference between the automatic compression and the manual which is as a result of inadequate compression, the results of the two systems in general for both manual and automatic compressions show that both systems thus FFDM and CRDM systems exert the forces within the acceptable limits in reference to the standing protocols stated by the IAEA's Human Health series for digital mammography thus the tolerance limit for the compression force is ± 20 N.

Table 4.3: Results of the compression force test for all five (5) systems

Mammography Systems	Compression Force (± 20 N)		Remarks Pass/Fail
	Automatic Compression	Manual Compression	
A	4	3	Pass
B	3	2	Pass
C	5	5	Pass
D	9	4	Pass
E	2	3	Pass

4.2.5 Tube Voltage Accuracy and Repeatability

This test was carried out in the quest to evaluate the accuracy and repeatability of the tube voltage at a constant kVp concerning the recommended tolerance limit of ±5 % by the IAEA's Human Health Series 2 for the tube voltage accuracy, whiles ≤5 % tolerance limits for the tubes voltage repeatability's difference and coefficient of variance (COV) respectively (IAEA 2009). It is indicative that all the five (5) mammography systems used for this study passed the tube voltage

accuracy and repeatability tests respectively implying the precision, reliability and accuracy of the tube voltage for mammography examinations. The voltage accuracy and repeatability are presented in Table 4.4 and derived from Appendix F.

Table 4.4: Results of the tube voltage accuracy and repeatability for the systems

Mammography Systems	kVp Accuracy (%)	kVp Repeatability at 28 kVp	
		COV (%)	Difference (%)
A	0.4	0.15	0.03
B	2.69	0.15	0.24
C	0.12	0.23	0.43
D	1.85	0.18	0.18
E	2.18	0.07	0.07

4.2.6 Output Repeatability and Linearity

For the accepted tolerance limit for output repeatability of ≤ 5 % for both the difference and for COV as recommended by the IAEA's Human Health Series (HHS) number 2, it can be stated that all five (5) mammography systems used for the study have passed the output repeatability test. The tolerance limit for the linearity test as stated by the IAEA's HHS number 2 is 10 % and all the understudied mammography systems passed this test indicating that the exposures is repeatable and constant at any mAs. Table 4.5 shows the output linearity results which is derived from Appendix G.

Table 4.5: Results of the output repeatability and linearity test for the mammography systems

Mammography Systems	Output Repeatability (%)		Output Linearity (%)
	Difference (%)	COV (%)	L
A	0.17	0.85	0.02
B	0.09	0.13	0.16
C	0.2	0.08	0.11
D	0.2	0.08	0.14
E	0.03	0.18	0.01

4.2.7 Half Value Layer test

This test was performed to confirm the appropriate quality of the radiation beam and to determine whether or not the total filtration is working perfectly. The HVL figures were calculated for all five (5) mammography systems at 28 kVp and 50 mAs. The results compared to the IAEA's HHS number 2, indicates that except for the system D which failed the HVL test, all the other four (4) mammography systems thus A, B, C and E passed the half value layer test indicating that the radiation beam quality is accurate and consistent and will produce maximum quality images but not in the system D where both weak and strong radiations will be exposed to the patient hence increasing patient dose whiles producing low quality images. Table 4.6 shows the half value layer test results and the raw data for the result is presented in Appendix I.

Table 4.6: Results of HVL tests for the mammography systems

Mammography Systems	HVL (mmAl) (kVp/100+0.03 ≤ HVL ≤ kVp/100+c)	PASS/FAIL
A	0.58	Pass
B	0.55	Pass
C	0.45	Pass
D	0.20***	Fail
E	0.41	Pass

*** indicates the results that are out of the tolerance limit

4.2.8 Timer Repeatability, Time and Tube Voltage Linearity

The timer repeatability was measured to confirm the accuracy, reproducibility and linearity of the X-ray tube output rate. They are relevant clinically regarding recommended standards (Yaffe *et al.*, 2006) and its coefficient of variance (COV) does not exceed the ≤ 2 % mark whiles the R^2 > 0.9 for the time and tube voltage linearities respectively. The results of this test are presented in Table 4.5 which shows that except for D systems which failed the time repeatability test, all the other four mammography systems thus A, B, C and E passed the time repeatability test. The results also show that the exposure time in the four mammography systems is highly reliable and the X-ray tube output does not vary over long periods. Also, from Table 4.7, it is indicative that all five mammography systems passed the time and tube voltage linearity tests respectively showing the consistency in the variation of the two parameters. The data for the time repeatability test was derived from Appendices I and J respectively.

Table 4.7: Results of other QC tests on the mammography systems

Mammography Systems	Time Repeatability COV (%) ≤ 2%	PASS/FAIL	Time Linearity ($R^2 > 0.9$)	kVp Linearity ($R^2 > 0.9$)	PASS/FAIL
A	0.07	Pass	0.97	0.99	Pass
B	0.24	Pass	0.99	0.99	Pass
C	0.08	Pass	0.99	0.99	Pass
D	8.64***	Fail	0.99	0.99	Pass
E	0.61	Pass	0.96	0.99	Pass

*** indicates the results that are out of the tolerance limit

4.3 Qualitative Image Quality and Lesion Detection Assessment

Achieving and assessing image quality in mammography has often been confronted with abiding challenges. The lasting link between clinical image quality and the high possibility of lesion detection is inevitable (Sosu *et al.*, 2018). The ACR phantom used in this study simulates and mimics a 4.2 cm breast whose thickness was kept constant. Figure 4.1 is the DICOM image of the ARC-MAP used in this study. The scoring of the DICOM images produced at varying technique factors concerning fibers, specks and masses embedded within the ACR phantom was done using the IAEA's recommended tolerance levels of ≥ 4 for fibers, ≥ 3 for both specks and masses respectively. Tables 4.8, 4.9 and 4.10 present the results of the scoring of inserts; thus fibers, specks and masses in the ACR phantom imaged using both the FFDM and CRDM systems from all the five mammography systems used in this study at varying technique factors. For the fiber detection results presented in the Table 4.8, both the FFDM and CRDM systems failed to meet the tolerance level at the lower technique factors of 26 kVp on 32 mAs for detecting fibers greater or equal to

four indicating the inadequate amount of radiations released as a result of lower technique factors used. At the 28 kVp on 40 mAs, the CRDM's system E exhibited higher fiber detection abilities over the two FFDM systems although the FFDM systems also passed the fiber detection at this selected technique factor.

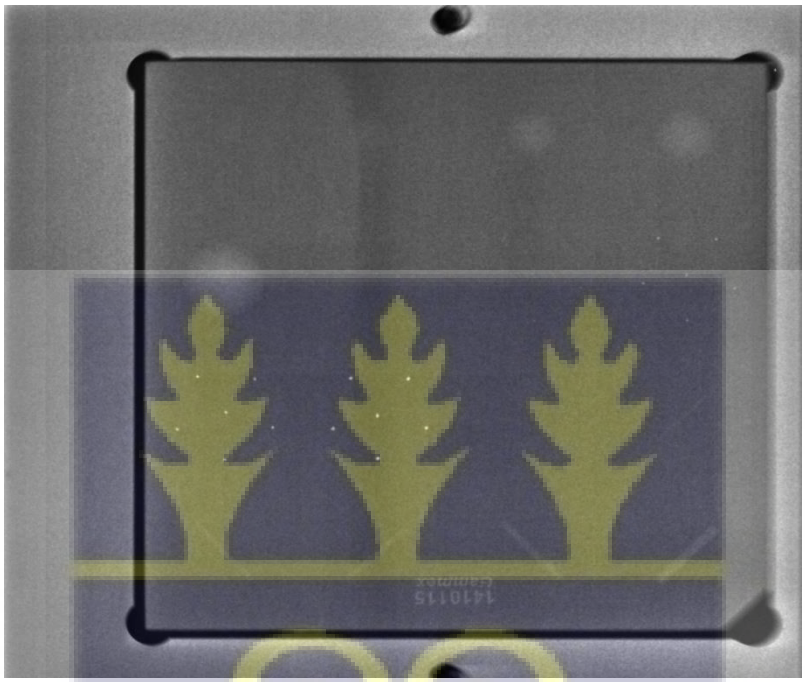

Figure 4.1: Image of the ACR MAP (Field Work)

The other two CRDM systems, C and D failed to pass the fiber detection at this selected technique factor. Also, at the 29 kVp on 50 mAs, system E (a CRDM) and systems A and B (FFDM systems) passed the fiber detection at this energy level with all the three systems scoring/detection four fibers respectively whiles the systems C and D of the CRDM systems failed to detect the recommended number of fibers at this selected technique factor. At the two highest selected technique factors used for this study, both the CRDM and FFDM systems passed the fiber detection with system A detecting the exact achievable number of (six) fibers within the ACR

MAP. Within the 30 kVp on 32 mAs and the 32 kVp on 130 mAs, the FFDM systems on the average detected 0.2 and 1.42 more fibers compared to the CRDM system respectively. Generally, the quality of the images with respect to their fiber detection increased with increased technique factors as shown in Table 4.8. It is also observed that the FFDM systems on the average saw a higher fiber detection of about 13 % more than the detection in the CRDM systems.

Table 4.8: Results of FFDM and CRDM fiber detections

kVp/mAs	Fiber detection within the mammography systems (≥ 4)				
	FFDM		CRDM		
	A	B	C	D	E
26/32	3.0	3.5	3.0	1.5	3.0
28/40	4.5	4.0	3.5	1.5	5.5
29/50	4.0	4.0	2.5	3.5	4.0
30/90	4.5	4.5	4.0	4.0	5.0
32/130	6.0	5.5	4.5	4.0	4.5

The specks detection abilities presented in Table 4.9 shows that specks detection within both the CRDM and the FFDM systems was increasing at increasing technique factors although systems A, D and E present some fluctuations at respective technique factors. The specks detected at the 26 kVp on 32 mAs was within the recommended limit for the two FFDM systems thus A and B and the CRDM's system E, where all the above-mentioned systems detected the same number of specks i.e., 3.5 specks respectively. The CRDM's system C and D failed the specks detection test detecting 2.5 and 1.0 specks respectively lower than the recommended ≥ 3 specks. Similarly, the CRDM's systems D and E failed the speck detection at 28 kVp and 40 mAs with systems A and

B of the FFDM systems and system C of the CRDM system passing the specks detection test. Both FFDM systems A and B, two systems from the CRDM systems C and E passed by detecting 4.0 and 3.5 specks within the two systems respectively at 29 kVp on 50 mAs whiles system D of the CRDM failed by detecting 2.0 specks. The two digital systems exhibited strong specks detection abilities at the technique factors of 39 kVp on 40 mAs, although all the five systems (FFDM and CRDM) passed the speck detection at this energy level, four out of the five systems thus A, B, C and D detected 4.0 specks whiles system E detected 3.0 specks. The narrative is the same for both systems at 23 kVp on 130 mAs with the exception on the CRDM's system which though passing varied with the detection of 3.5 specks. Aside the few similarities within the specks detection, it is indicative that, the possibilities of detecting speck-like lesions within the FFDM systems are highly achievable compared to the possibilities of same within the CRDM with all the available technique factors. The data in Tables 4.8, 4.9 and 4.10 were derived from Appendix K.

Table 4.9: Results of FFDM and CRDM specks detections

kVp/mAs	Specks detection within the mammography systems (≥ 3)				
	FFDM		CRDM		
	A	B	C	D	E
26/32	3.5	3.5	2.5	1.0	3.5
28/40	3.0	3.5	3.0	1.5	2.5
29/50	4.0	3.5	4.0	2.0	3.5
30/90	4.0	4.0	4.0	4.0	3.0
32/130	4.0	4.0	4.0	3.5	3.0

The detection of masses within the ACR phantom is presented in Table 4.10 below where the results of all the five mammography systems both the CRDM and the FFDM are discussed. At the 26 kVp and 32 mAs, whiles only one FFDM system passed the test i.e., system B detecting 3 masses, all the CRDM systems failed the mass detection at this energy with system D detecting as low as 1.0 mass inserts. At 28 kVp and 40 mAs on the other hand, while only system D passed within the CRDM systems, C and E failed to detect up to the recommended limit. However, the two FFDM systems passed the mass detection at this energy level. At 29 kVp and 50 mAs level, all the FFDM and CRDM systems passed the mass detection test and exhibited equal detection of masses with alternating scores of 3.5 and 4.0 respectively. Both FFDM and CRDM systems passed the mass detection at 30 kVp and 90 mAs and 32 kVp and 130 mAs with the FFDM on each respective energy level producing better detection on the average compared to the CRDM systems.

Table 4.10: Mass detection within the FFDM and CRDM systems

kVp/mAs	Mass detection within the mammography systems (≥ 3)				
	FFDM			CRDM	
	A	B	C	D	E
26/32	2.5	3.0	2.0	1.0	2.5
28/40	3.0	3.0	2.5	3.5	2.5
29/50	3.5	4.0	3.5	4.0	3.5
30/90	4.5	4.5	3.0	3.0	4.0
32/130	4.5	4.5	4.0	4.0	4.5

Generally, the FFDM systems present relatively higher possibilities of detecting fibers, specks and masses indicating the increased probabilities of lesion detection within the FFDM systems (Brooks

et al., 1997) compared to the CRDM systems. The IAEA's Human Health Series Numbers 2 and 17 recommends that the total score for an ACR phantom in the image quality assessment must be greater than 10 (> 10) thus the accumulative score of fibers, specks and masses (IAEA, 2011). Table 4.11 presents the total score from the CRDM and FFDM systems used in this study in the respective varying technique factors. From Table 4.11, irrespective of the rise in total detection with increasing technique factors within both systems, all the mammography systems both in the CRDM and the FFDM systems accumulatively failed to reach the tolerance limit score at the 26 kVp on 32 mAs. There appears to be a steady increase in total score at the 26 kVp on 32 mAs and at 28 kVp on 40 mAs respectively resulting in all the FFDM systems i.e. A and B, and the CRDM system E passing the tolerance limit with an equal score of 10.5 within the three systems. While indicating an increase in the detection of lesions at an increased technique factors, systems C and D failed to meet the limit scoring a total of 9.0 and 6.5 respectively. At the 29 kVp on 50 mAs, the narrative above is the same for the five systems, where systems A and B of the FFDM passed with 11.5 each, a 1.5 more detection with reference to the tolerance limit. Within the CRDM on the other, only the system E passed with 11.0 score a 1.0 more detection whiles both systems C and D failed to meet the greater than 10 marks.

Table 4.11: Overall summary score of both the FFDM and CRDM systems

kVp/mAs	Total detection within the systems (> 10)				
	CRDM			FFDM	
	A	B	C	D	E
26/32	9	10	7.5	3.5	9
28/40	10.5	10.5	9	6.5	10.5
29/50	11.5	11.5	10	9.5	11
30/90	13	13	11	11	12
32/130	14.5	14	12.5	11.5	12

Again, from Table 4.11, both the FFDM and CRDM systems passed the tolerance score limit at 30 kVp on 90 mAs and 32 kVp on 130 mAs respectively although the FFDM shows higher detection abilities detecting as high as 13 and 14.5 inserts at the respective energy levels. System D in the CRDM systems showed lower possibilities of detection even at higher technique factors and requires further investigation to ascertain why. Both the CRDM and FFDM systems used in the study showed similar trends with increasing technique factors. The FFDM systems on the average proves superior to the CRDM systems by detecting some 17.7 % more at the 26 kVp on 32 mAs, and amongst all the technique factors used, the FFDM systems detected an 11.4 %, 8.3 %, 10.6 % and a 14.1 % down the table while the technique factors were increasing. This indicates that the FFDM system at any given energy may produce high-quality images whiles enhancing higher lesion detectability compared to the CRDM systems. Figure 4.2 shows the percent visibility evaluated on all the total detections within the FFDM and CRDM systems used for the study. From the graph, the FFDM systems indicates highest visibility of up to 90 % over the CRDM's highest

of about 78.1 % relative to their lowest respective percent visibilities of 62.5 % to 21.9 %. The FFDM's lesion detection abilities are superior to that of the CRDM systems.

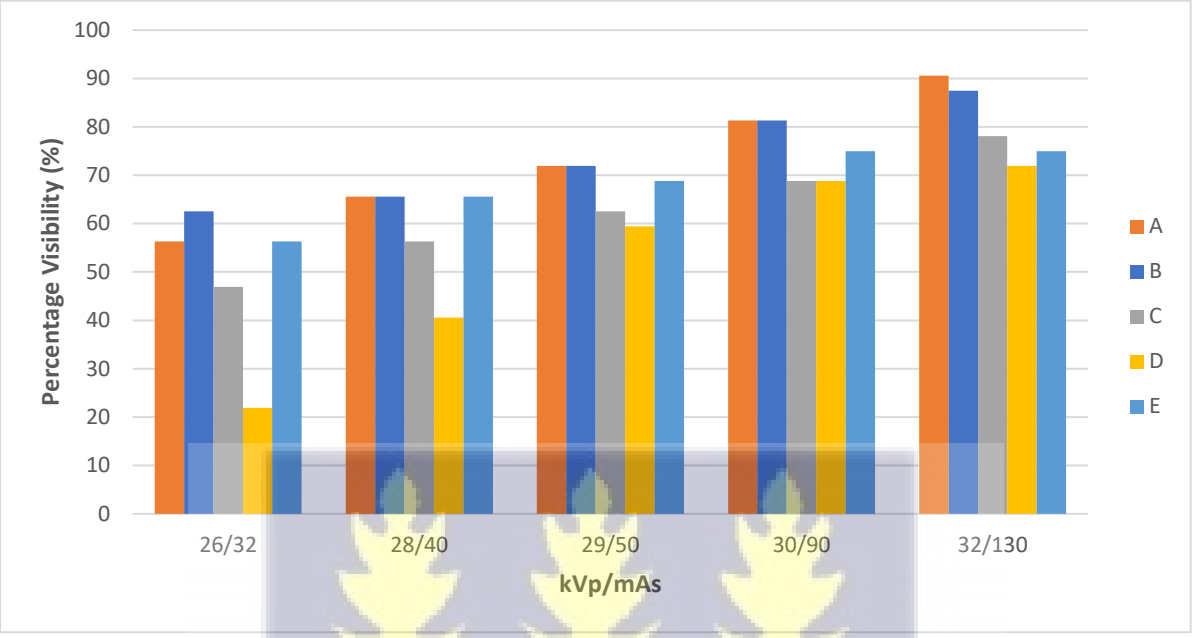

Figure 4.2: Graph of the percentage visibility against varying kVp and mAs

4.4 Quantitative Image quality Assessment

4.4.1 Detectability and Spatial Resolution

The fineness of spatial detail that an imaging system can demonstrate or resolve is directly related to the maximum quality of the image and the maximum efficiency of the imaging system. This test was performed to verify whether the spatial resolution of the imaging system has not deteriorated whiles improving image interpretation and the level of confidence for easier detection of microcalcifications among the various imaging systems and their users. The measure of spatial resolution pattern is done in terms of the number of line pairs per millimeter (lp/mm) and must be excellent to reveal the calcifications, their number and their shape within the breast. According to

the IAEA's HHS numbers 2 and 17, the achievable tolerance should be ≥15 lp/mm in both directions whiles the acceptable tolerance should be ≥11 lp/mm in both directions. From the results presented in Table 4.12 where measurements were made at constant 29 kVp for the 20 mm PMMA thickness whiles increasing mAs, it was observed that the spatial resolution increases steadily with an increase in the mAs used. At 30 mAs within this PMMA thickness, all the FFDM and CRDM systems failed to meet the acceptable tolerance limit for the spatial resolution test although the systems B of FFDM and system E of the CRDM systems were close with 10 lp/mm. At 30 mAs within this PMMA thickness, all the CRDM systems failed the test whiles one of the FFDM systems i.e., system B passed scoring 11 lp/mm. At 90 mAs within the same thickness, both the FFDM systems passed the test with system B reaching the achievable limit whiles only one of the CRDM systems passed this test i.e., system E. All the FFDM and CRDM systems passed the spatial resolution test at the 120 mAs and 150 mAs respectively with the FFDM systems reaching the achievable limits mark as high as 16 lp/mm over the CRDM's high tolerance limit score of 13 lp/mm. The FFDM systems outperformed the CRDM system in the spatial resolution test at the 20 mm thickness with accumulative averages of 0.33 lp/mm, 1.83 lp/mm, 3.50 lp/mm, 3.83 lp/mm and 4.33 lp/mm in the respective increasing other of the mAs' used. It is inductive that, down the Table as the mAs increases, the spatial resolution increases hence an increase in the quality of images produce and the increase in the lesion detectability and the FFDM systems showed superior performance over the CRDM systems.

Table 4.12: Results of the spatial resolution test at 29 kVp and 20 mm

mAs	Spatial Resolution at 29 kVp and 20 mm				
	FFDM		CRDM		
	A	B	C	D	E
30	7	10	5	5	10
60	10	11	8	8	10
90	12	15	10	9	11
120	15	16	11	12	12
150	16	18	13	12	13

Although the measuring conditions used for this study may slightly vary from the exposure parameters used in some diagnostic settings, the respective parameters necessary for quality images are unchanged. It is seen from Table 4.13, all the FFDM and CRDM systems used for the study failed to detect the recommended limits at the 30 mAs for the constant 29 kVp and the 45 mm PMMA thickness. Similarly, all the systems failed at the 60 mAs although the CRDM's system E score as close as 10 lp/mm. Both the FFDM and CRDM system exhibit closeness in spatial resolution for the 45 mm thickness at the 90 mAs level although all the five systems failed the test at this level. The un-doubted increase in the spatial resolution with increasing mAs makes one to expect that the system will meet the tolerance limit at 120 mAs and 150 mAs respectively, yet the FFDM's system A and the CRDM's system D failed at 120 mAs and system D failed with 10 lp/mm at 150 mAs. Whiles the spatial resolution decreased at the 45 mm compared to that of the 20 mm, the CRDM systems on the average detected better than the FFDM at the 45 mm with a 0.17 lp/mm average difference at the 30 mAs and 60 mAs' respectively. At the 90 mAs, 120 mAs and 150 mAs', the average difference of the CRDM to the FFDM in the spatial resolution is

0.1 lp/mm, 1.07 lp/mm and 0.5 lp/mm respectively. The CRDM systems show superiority over the FFDM systems in spatial resolution at the 45 mm PMMA thickness.

Table 4.13: Results of the spatial resolution test at 29 kVp and 45 mm

mAs	Spatial Resolution at 29 kVp and 45 mm				
	FFDM		CRDM		
	A	B	C	D	E
30	5	6	5	4	8
60	8	7	8	5	10
90	10	9	10	9	10
120	10	11	12	9	11
150	12	11	14	10	12

The behavior of the FFDM and CRDM systems concerning the increasing mAs and PMMA thickness at a constant kVp of 29 kVp is in no way different. From Table 4.14, it is generally observed that the readable lp/mm scores increase down the Table with increasing mAs whiles on the other hand, the readable lp/mm scores decrease with increasing PMMA thickness. Concerning the tolerance limit of the readable lp/mm scores of ≥11 lp/mm as recommended, all the FFDM failed the test and the various mAs' whiles only the system E of the CRDM systems passed the spatial resolution test with a score of 11 lp/mm leaving the rest of the CRDM systems failing the test. On the cumulative average, the CRDM systems perform better in the higher thickness with respective averages of 4.0 lp/mm, 0.67 lp/mm, 0.17 lp/mm, 1.33 lp/mm and 1.5 lp/mm against the used mAs'. Although the average detection within the CRDM appear to be better than that of the FFDM within the 45 mm and 70 mm respectively, many of its readable detections could not meet

the recommended tolerance limits hence the need for appropriate compression to enhance the image quality and detection. Also, a simultaneous increase in the technique factor will give maximum quality whiles enabling detectability (Noel & Thibault, 2004). Figure 4.3 is a DICOM image of the TORMAS phantom used in this study.

Table 4.14: Results of the spatial resolution test at 29 kVp and 70 mm

mAs	Spatial Resolution at 29 kVp and 70 mm				
	FFDM		CRDM		
	A	B	C	D	E
30	4	2	4	3	7
60	5	5	6	4	7
90	6	7	6	6	8
120	6	8	7	8	10
150	9	8	10	9	11

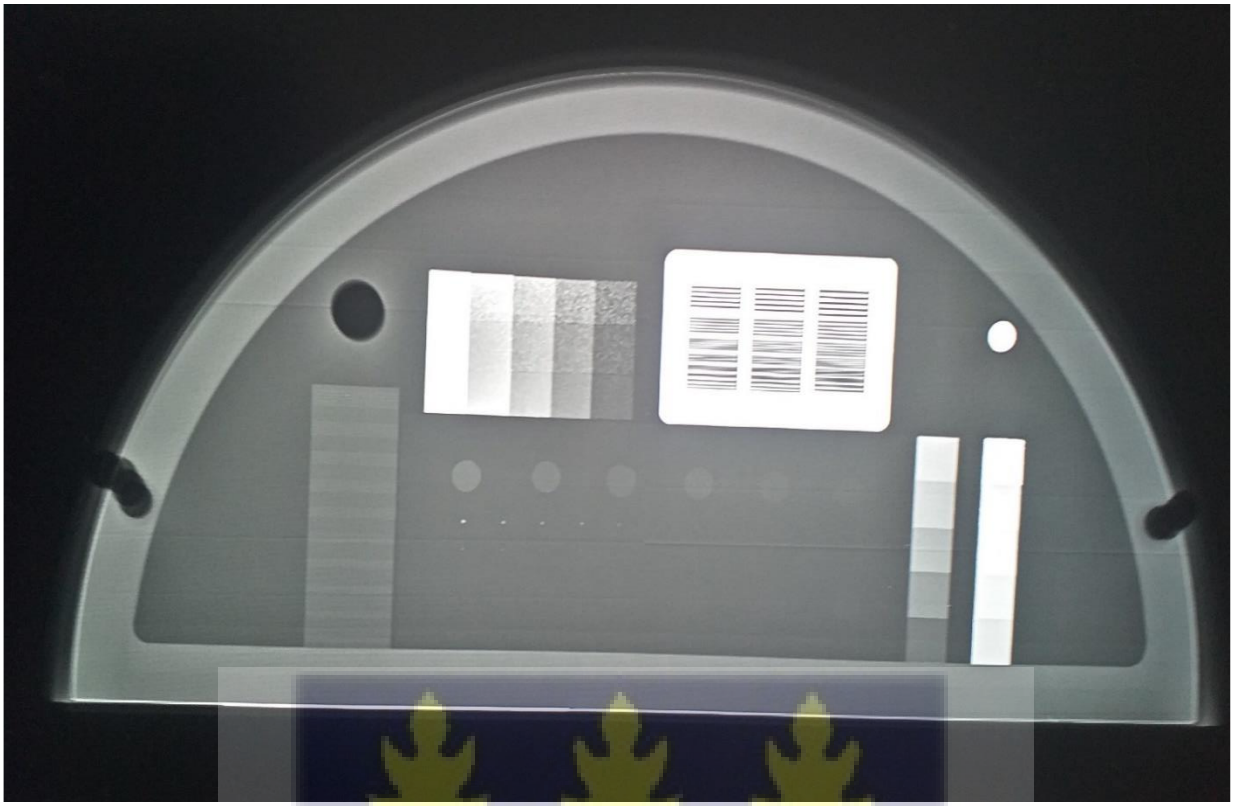

Figure 4.3: An image of the TORMAS phantom (Field Work)

4.4.2 Spatial Resolution at Varying kVp

The importance of compression to image quality plays a maximum role in the detectability of lesions in mammography. Results from table 4.15 at a constant 50 mAs and 20 mm PMMA thickness shows that at the 26 kVp, all the two FFDM systems passed the spatial resolution test with a 3.5 lp/mm more on the average than the CRDM systems which all failed to meet the tolerance limit mark. Similarly, at the 28 kVp, all the FFDM systems passed while the CRDM systems on the other hand failed with the FFDM averagely detecting about 4.2 lp/mm more than in the CRDM systems. The FFDM systems at the 29 kVp exceeded the recommended tolerance limit to the recommended achievable limits which indicate the maximum detection abilities of the system compared to the CRDM system where two out of the three systems passed the test whiles

system D fails to meet the tolerance limit. The FFDM exhibits a 4.7 lp/mm more detection abilities over the CRDM systems, an indication of the production of quality images comparatively. At the 30 kVp, both FFDM and CRDM systems passed the test with the FFDM systems again reaching the achievable limits exhibiting some 3.5 lp/mm more abilities over the CRDM systems. Similar abilities were exhibited by both systems at the 32 kVp energy level, where the FFDM systems and two CRDM systems reached the achievable limits of detection with only the system D of the CRDM systems reaching the tolerance limit. Although the two systems exhibit excellent detection abilities at this energy level, the FFDM systems continue to exhibit superiority with some 4.5 lp/mm detection ability over the CRDM systems.

Table 4.15: Results of spatial resolution at 50 mAs and 20 mm.

kVp	Spatial Resolution at 50 mAs and 20 mm				
	FFDM		CRDM		
	A	B	C	D	E
26	11	12	7	8	9
28	13	14	9	9	10
29	15	17	12	10	12
30	16	17	13	12	14
32	18	19	16	14	15

Results from Table 4.16 shows the behavior of both systems with respect to varying kVp and constant mAs of 50 mAs at the 45 mm PMMA thickness. At the 26 kVp, both FFDM and CRDM systems failed the test though the two FFDM systems and the system E from CRDM system show strong detection abilities. The two FFDM systems passed whiles only of the CRDM systems i.e.,

the system E, passed at the 28 kVp. Systems C and D failed at this energy level with 8 and 9 lp/mm respectively. At the 29 kVp and 30 kVp, both the FFDM and CRDM systems passed the tolerance limit with the FFDM exhibiting superiority over the CRDM system achieving spatial resolution scores average 2.2 lp/mm and 1.5 lp/mm more than that of the CRDM systems, an indication of good quality image production within the FFDM systems. Again, at the 32 kVp, all the FFDM and CRDM systems passed the test whiles system D from the CRDM systems had the lowest spatial resolution value, the FFDM system exceeded the tolerance limit to the achievable limit exhibiting some 2.5 lp/mm more detection abilities over the CRDM systems.

Table 4.16: Results of spatial resolution at 50 mAs and 45 mm.

kVp	Spatial Resolution at 50 mAs and 45 mm				
	FFDM		CRDM		
	A	B	C	D	E
26	10	10	7	8	10
28	11	13	8	9	11
29	13	14	11	12	11
30	13	14	12	12	12
32	15	16	13	12	14

Table 4.17 below shows the results of the spatial resolution test at constant 50 mAs and 70 mm PMMA thickness whiles varying the kVp. From the table, both the FFDM and CRDM systems failed the test at the 26 kVp but the CRDM's system E exhibits a strong detection ability. At the energy level, the average score difference between the systems indicates that the FFDM system remains superior. At the 28 kVp, only one of the FFDM system passed i.e., system B whiles all

the CRDM systems failed to meet the recommended limits. All the FFDM systems passed at 29 kVp whiles two systems from the CRDM system passed with the system D failing the test, here the FFDM exceeds the CRDM with an average of 1.83 lp/mm more detections. Both the FFDM and CRDM systems passed the spatial resolution test at the 30 kVp and 32 kVp respectively. Again, the FFDM system exhibit maximum quality and detection abilities over the CRDM systems with a 1.33 lp/mm and 1.70 lp/mm more of detection. Above all, the spatial resolution increases as the technique factors increase but decreases as the thicknesses increase. This however requires an intentional effort on adequate compression before exposures are made. There is the need for regulatory attention for system D to access its effectiveness in the production of quality images.

Table 4.17: Results of spatial resolution at 50 mAs and 70 mm.

kVp	Spatial Resolution at 50 mAs and 70 mm				
	FFDM			CRDM	
	A	B	C	D	E
26	8	8	6	7	10
28	9	11	9	8	10
29	12	13	11	10	11
30	12	14	12	11	12
32	13	15	12	12	13

4.4.3 Signal-to-Noise Ratio Analysis

The high standards of image quality and equipment performance in mammography are inevitably relevant in the detection of lesions since the breast tissues and pathological findings have very

close linear attenuation coefficients within lower energy ranges as used in mammography. Image quality in a digital system is commonly defined in the system's ability to detect inserts in an unsuspecting region. According to Albert Rose, there exists a relationship between direct proportionality between the quality of an image and its correlation to the signal-to-noise stating a tolerance limit of greater than 5 (Burgess, 1999) such that, a system's ability to produce spatial particles of interest in an image is expected to be good should the signal-to-noise ratio is greater than 5. This however contradicts the standard in screen film, thus contrast can easily be manipulated in digital images to achieve highly desired contrast (Samei *et al.,* 2005; Samei *et al.,* 2008), hence contrast is not the peculiar parameter for image quality assessment making room for a more relevant measure of quality by using the signal-to-noise ratio (SNR) and the digital image with a higher level of SDNR could provide inherently superior image quality (Kawashima *et al.,* 2017). Regions of interest were drawn on the DICOM images using the ImageJ software and the necessary mean pixel values within the ROIs were measured for the calculation of the system's signal-to-noise ratio amongst the used PMMA thicknesses thus 20 mm, 45 mm, and 70 mm respectively. The calculated SNR values are shown in Table 4.18 and derived from Appendix L.

Table 4.18: Calculated SNR for the five (5) systems used

Mammography Systems	**PMMA thicknesses**		
	20 mm	**45 mm**	**70 mm**
A	11.01	8.67	5.12
B	12.07	9.59	5.17
C	10.04	7.60	2.63
D	6.96	2.57	1.01
E	8.03	6.24	4.96

Results presented in Table 4.18 show that all five systems i.e., FFDM and CRDM systems used for this study have good SNR at the 20 mm PMMA thickness though the system D of CRDM systems had the lowest SNR value of 6.69. Within the 20 mm thickness, the FFDM systems accumulated the highest calculated values of SNR against the CRDM. On the average, the FFDM system's SNR value was 3.2 times more than that of the CRDM hence its ability to detect better and produce higher quality images. With the decrease in SNR as the PMMA thickness increases, all the FFDM and CRDM systems saw a steady decrease in the calculated SNR value at the 45 mm thickness with the system D of the CRDM systems falling below the recommended limit i.e., SNR value of 2.57. The FFDM systems tend to accumulate the higher SNR values and a 3.66 SNR more on the average against the CRDM systems. At the 70 mm thickness also, the steady decrease in the calculated SNR values was evident with only the FFDM systems passing the SNR test whiles all the CRDM systems failed. On the accumulative average, the FFDM systems had a 2.28 more SNR value than the CRDM system indicating the possible abilities of the FFDM system to produce quality images and higher detection abilities at higher thicknesses. The SNR values of the FFDM systems indicate the systems superiority in the production of quality images compared to images produced by the CRDM systems. The results also provide evidence of the impact of adequate compression on image quality (Chevalier *et al.*, 2012; Sosu 2018) that when the thickness is reduced at maximum, producing a quality image is inevitable. Figure 4.4 is the DICOM image of the PMMA slab sandwiched with an Aluminum filter and indication the ROIs.

The study was conducted in five diagnostic radiology departments with mammography centers in the Greater Accra region of Ghana. It was a phantom-based study and subjected to only five out of the many mammography facilities in the region. The limitation to this study was mainly the hard nature of the phantom used to mimic the breast. This made compression difficult without considerations to the motion in normal cases. It also made it impossible for most of the underlined

inserts in the phantom to be effectively imaged/viewed. Moreover, the fact that the objects in the phantom are only arranged at one specific depth so that neither the reconstruction depth nor the object visibility at different depths can be analyzed. This study is also unable to account for the breast density variations and the effect of dose on the image quality produced.

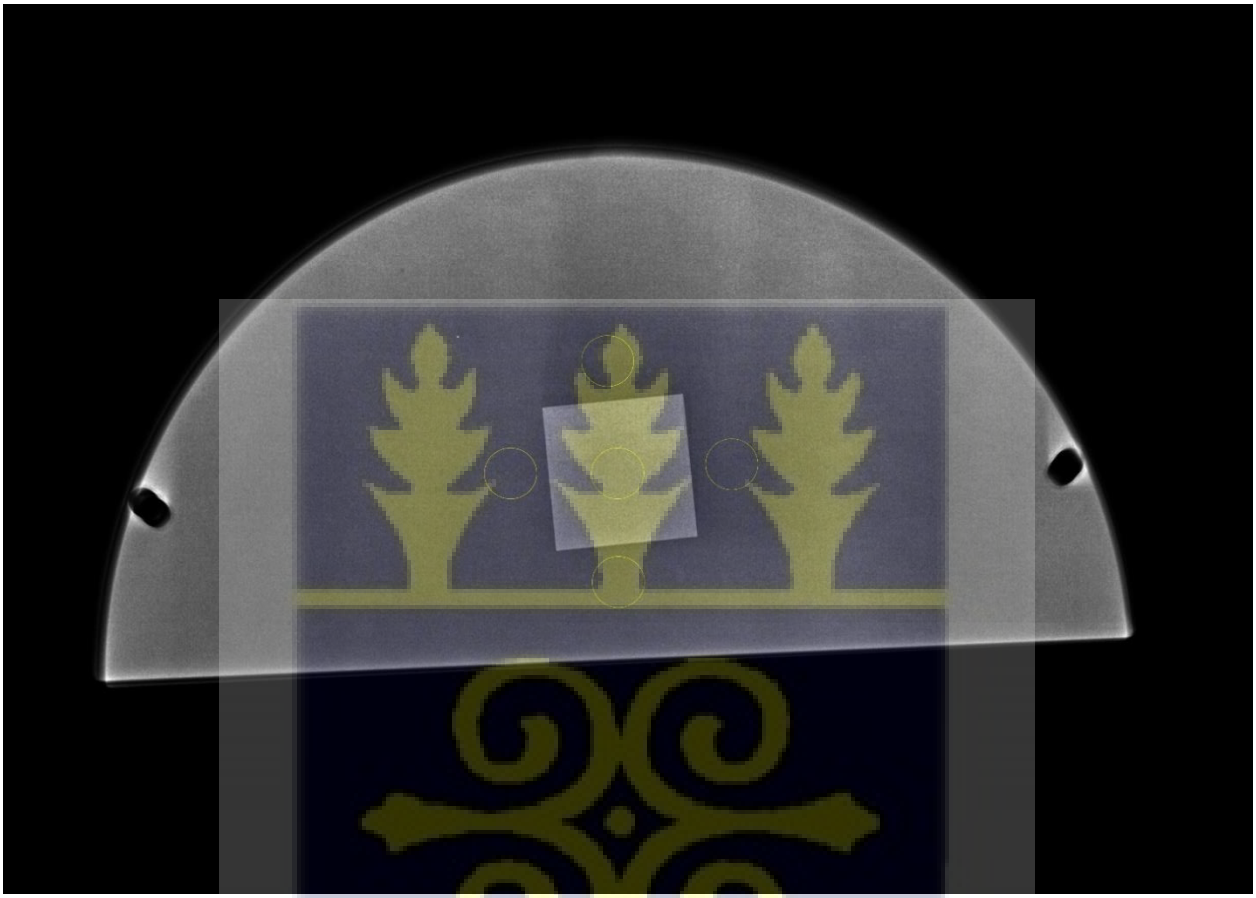

Figure 4.4: ROI's drawn in the PMMA phantom sandwiched with an Aluminum filter (Field Work)

CHAPTER FIVE

CONCLUSION AND RECOMMENDATIONS

5.1 Pre-Exposure and Exposure Performance

Apart from D amongst the CRDM systems which failed the HVL test, all the other pre-exposure and exposure performance tests results obtained from the other systems were within the internationally recommended acceptable levels. This, however, implies that four out of the five mammography machines used for the study were functioning adequately. The HVL result of the system D was below the recommended limit hence the poor quality and detection exhibited in most of the results of that facility. All the mammography systems used for the study have a working DICOM setup.

5.2 Qualitative Image Quality Assessment

Both FFDM and CRDM systems produced quality images qualitatively yet proportional to increasing the detectability as the technique factors (kVp and mAs) increased. However, the FFDM system was superior to the CRDM and produced a more satisfactory or better-quality images compared to the CRDM systems. This also showed in the higher detection of lesions in the FFDM systems over the CRDM.

5.3 Quantitative Image Quality Assessment

The signal-to-noise ratio (SNR) results indicate that adequate good quality image is achievable at the 20 mm and 45 mm thicknesses within both the CRDM and FFDM systems respectively but decreased quality at 70 mm. Signal-to-noise ratio decreases with increasing PMMA thickness

whiles the FFDM system showed the potential of better quality over the CRDM systems with reference to the SNR values.

The spatial resolution as an image quality parameter estimated within the systems used for this study indicates that the FFDM systems recorded acceptable resolutions for the 20 mm and 45 mm thicknesses at higher mAs values respectively indicative of good quality images while the resolution at the 70 mm thickness was unsatisfactory with the production of relatively poorer quality images. Within the CRDM systems, the C and E systems produced fairly good quality images with satisfactory spatial resolutions across the various thicknesses whiles the system D indicates poorer image qualities about its estimated spatial resolution. The same observations were made for spatial resolution at varying kVp for both the FFDM and the CRDM systems. In all, the FFDM system provided better spatial resolution and better image quality relative to the CRDM.

5.4 Recommendations

The following recommendations are being made for consideration by the following stakeholders: Ministry of Health/Ghana Health Service, Medical Physicists, and Radiographers.

5.4.1 Ministry of Health/Ghana Health Service and Hospital Authorities

i. The adaptation and enforcement of the adherence to the Quality Control protocol established for the African region are recommended to authorities. It is also recommended that the MoH/GHS employ medical physicists and make the same mandatory for private facilities to ensure regular quality control and quality assessment and the adequate functioning of medical/imaging equipment.

ii. Follow-up and risk assessment should be done on the system D, since most of its outcomes were below the acceptable range.

5.4.2 Medical Physicists

The following are recommended for consideration of the medical physicist:

i. that the medical physicist should ensure that the necessary quality control tests and daily checks are conducted to ensure proper functioning of equipment,

ii. that the medical physicist should ensure that only optimized procedures and parameters are used.

5.4.3 Radiographers

i. It is recommended that adequate compression is applied before any exposure is made to the breast whiles promptly reporting any faulty compression system to authorities for immediate actions to be taken. Also, radiographers using the manual modes of exposure are encouraged to do due diligence in the selection of technique factors for exposures to the breast.

ii. Technique factors for optimal detection outcome and image quality at any breast thickness should be 28 kVp and 50 mAs respectively for FFDM, then 29 kVp and 50 mAs for CRDM systems.

5.4.4 Further Studies

i. With the inclusion of the breast tomosynthesis system in the mammography practice in Ghana, the extension of this study can be undertaken to compare the quality of detection between the FFDM and the breast tomosynthesis systems.

REFERENCES

American Cancer Society (2022). *Cancer Facts & Figures 2022| American Cancer Society*. Retrieved on 12th June, 2022, from https://www.cancer.org/research/cancer-facts-statistics/all-cancer-facts-figures/cancer-facts-figures-2022.html

American Cancer Society (2020). *Cancer Facts and Figures 2020| American Cancer Society*. Retrieved from https://www.cancer.org/content/dam/cancer-org/research/cancer-facts-and-statistics/annual-cancer-facts-and-figures/2020/cancer-facts-and-figures-2020.pdf on August, 2022

American College of Radiologist, (2019). Phantom Testing: Mammography, Accreditation Support. Retrieved on 12th May, 2022 from https://accreditationsupport.acr.org/support/solutions/articles/11000065938-phantom-testing-mammography-revised-12-12-19-

Adesunkanmi, A. R. K., Lawal, O. O., Adelusola, K. A., & Durosimi, M. A. (2006). The severity, outcome and challenges of breast cancer in Nigeria. *The Breast*, *15*(3), 399–409. https://doi.org/10.1016/j.breast.2005.06.008

Adjei, E. (2012). Breast cancer in Kumasi, Ghana. *Ghana Medical Journal*, *46*(1), Article 1. https://doi.org/10.4314/gmj.v46i1

Albrektsen, G., Heuch, I., & Kvåle, G. (1995). The short-term and long-term effect of pregnancy on breast cancer risk: A prospective study of 802,457 parous Norwegian women. *British Journal of Cancer*, *72*(2), 480–484. https://doi.org/10.1038/bjc.1995.359

Anatomy of the Breasts. Figure 1. (2021, August 8). Retrieved on 02 June, 2022 from https://www.hopkinsmedicine.org/health/wellness-and-prevention/anatomy-of-the-breasts

Anderson, W. F., Jatoi, I., Tse, J., & Rosenberg, P. S. (2010). Male Breast Cancer: A Population-Based Comparison with Female Breast Cancer. *Journal of Clinical Oncology*, *28*(2), 232–239. https://doi.org/10.1200/JCO.2009.23.8162

Armstrong, K., Eisen, A., & Weber, B. (2000). Assessing the Risk of Breast Cancer. *New England Journal of Medicine*, *342*(8), 564–571. https://doi.org/10.1056/NEJM200002243420807

Biritwum B. R.,; Amaning A. O. (2000). Pattern of diseases or conditions leading to hospitalization at the Korle Teaching hospital, Ghana (1996). *Ghana Medicine Journal*, 197-205.

Bistoni, G., & Farhadi, J. (2015). Anatomy and physiology of the breast. In R. D. Farhadieh, N. W. Bulstrode, & S. Cugno (Eds.), *Plastic and reconstructive surgery* (pp. 477–485). John Wiley & Sons, Ltd. https://doi.org/10.1002/9781118655412.ch37

Bland, K. I., & Copeland, E. M. I. (1993). The Breast: Comprehensive Management of Benign and Malignant Diseases. *Plastic and Reconstructive Surgery*, *92*(5), 973–974.

Boquien, C. Y. (2018). Human Milk: An Ideal Food for Nutrition of Preterm Newborn. *Front. Pediatric*, *6*. Retrieved on 4th May, 2022 from https://www.frontiersin.org/articles/10.3389/fped.2018.00295

Bochud, F. O., Verdun, F. R., Valley, J.-F., Hessler, C., & Moeckli, R. (1997). Importance of anatomical noise in mammography; Medical Imaging. H. L. Kundel, Ed.; pp. 74–80. https://doi.org/10.1117/12.271313

Breastcancer.org. (2022). Breast Cancer Risk Factors. Retrieved on April, 2022 from https://www.breastcancer.org/risk/risk-factors

Brooks, K. W., Trueblood, J. H., Kearfott, K. J., & Lawton, D. T. (1997). Automated analysis of the American College of Radiology mammographic accreditation phantom images. *Medical Physics*, *24*(5), 709–723. https://doi.org/10.1118/1.597992

Burgess, A. E. (1999). The Rose model revisited. *Journal of the Optical Society of America A*, *16*(3), 633. https://doi.org/10.1364/JOSAA.16.000633

Campbell, L. L., & Polyak, K. (2007). Breast Tumor Heterogeneity: Cancer Stem Cells or Clonal Evolution? *Cell Cycle*, *6*(19), 2332–2338. https://doi.org/10.4161/cc.6.19.4914

Cancer Facts & Figures 2021 | American Cancer Society. Retrieved on September 16, 2022, from https://www.cancer.org/research/cancer-facts-statistics/all-cancer-facts-figures/cancer-facts-figures-2021.html

Cancer.org. (2020). *Physical Activity and the Person with Cancer*. Retrieved on September 16, 2022, from https://www.cancer.org/treatment/survivorship-during-and-after-treatment/be-healthy-after-treatment/physical-activity-and-the-cancer-patient.html

Carter, C., & Veale, B. (2022). *Digital radiography and PACS E-Book*. Elsevier Health Sciences. Pg. 226

CDCBreastCancer. (2022). *What Are the Symptoms of Breast Cancer?* Centres for Disease Control and Prevention. Retrieve on 5th September, 2022 from https://www.cdc.gov/cancer/breast/basic_info/symptoms.htm

Chevalier, M., Leyton, F., Nogueira, M., Oliveira, M., da Silva, T. A., & Emilio, J. (2012). Image Quality Requirements for Digital Mammography in Breast Cancer Screening. In L. Tabar (Ed.), *Imaging of the Breast—Technical Aspects and Clinical Implication*. *InTech*. https://doi.org/10.5772/30973

Coronado, G. D., Beasley, J., & Livaudais, J. (2011). Alcohol consumption and the risk of breast cancer. *Salud Pública de México*, *53*(5), 440–447.

Coughlin, S. S. (2019). Epidemiology of Breast Cancer in Women. In A. Ahmad (Ed.), Breast Cancer Metastasis and Drug Resistance: Challenges and Progress (pp. 9–29). *Springer International Publishing*. https://doi.org/10.1007/978-3-030-20301-6_2

Cramer, D. W. (2012). The Epidemiology of Endometrial and Ovarian Cancer. *Haematology/Oncology Clinics of North America*, *26*(1), 1–12. https://doi.org/10.1016/j.hoc.2011.10.009

Dance, D. R., Thilander, A. K., Sandborg, M., Skinner, C. L., Castellano, I. A., & Carlsson, G. A. (2000). Influence of anode/filter material and tube potential on contrast, signal-to-noise ratio and average absorbed dose in mammography: A Monte Carlo study. *The British Journal of Radiology*, *73*(874), 1056–1067. https://doi.org/10.1259/bjr.73.874.11271898

Dance, D. R., Skinner, C. L., Young, K. C., Beckett, J. R., & Kotre, C. J. (2000). Additional factors for the estimation of mean glandular breast dose using the UK mammography dosimetry protocol. *Physics in Medicine and Biology*, *45*(11), 3225–3240. https://doi.org/10.1088/0031-9155/45/11/308

Delen, D., Walker, G., & Kadam, A. (2005). Predicting breast cancer survivability: A comparison of three data mining methods. *Artificial Intelligence in Medicine*, *34*(2), 113–127. https://doi.org/10.1016/j.artmed.2004.07.002

DeSantis, C. E., Ma, J., Goding Sauer, A., Newman, L. A., & Jemal, A. (2017). Breast cancer statistics, 2017, racial disparity in mortality by state: Breast Cancer Statistics, 2017. *A Cancer Journal for Clinicians*, *67*(6), 439–448. https://doi.org/10.3322/caac.21412

DICOM. (2012). *DICOM*. DICOM. https://www.dicomstandard.org

Digital Radiography. (2021). In *Wikipedia*. Retrieved on 2nd February, 2022 from https://en.wikipedia.org/w/index.php?title=Digital_radiography&oldid=1058718214

Dumitrescu, R. G., & Cotarla, I. (2005). Understanding breast cancer risk—Where do we stand in 2005? *Journal of Cellular and Molecular Medicine*, *9*(1), 208–221. https://doi.org/10.1111/j.1582-4934.2005.tb00350.x

Dustler, M., Andersson, I., Brorson, H., Fröjd, P., Mattsson, S., Tingberg, A., Zackrisson, S., & Förnvik, D. (2012). Breast compression in mammography: Pressure distribution patterns. *Acta Radiologica*, *53*(9), 973–980. https://doi.org/10.1258/ar.2012.120238

Dzidzornu, E., Angmorterh, S. K., Ofori-Manteaw, B. B., Aboagye, S., Ofori, E. K., Owusu-Agyei, S., & Hogg, P. (2021). Compression force variability in mammography in Ghana – A baseline study. *Radiography*, *27*(1), 150–155. https://doi.org/10.1016/j.radi.2020.07.007

Eaton, L. (2002). Early periods and late childbearing increase the risk of breast cancer, a study confirms*: British Medical Journal*, *324*(7334), 386.

Erwin, D. O., Spatz, T. S., Stotts, R. C., Hollenberg, J. A., & Deloney, L. A. (1996). Increasing mammography and breast self-examination in African American women using the witness project. *Journal of Cancer Education*, *11*(4), 210–215. https://doi.org/10.1080/08858199609528430

Fackenthal, J. D., & Olopade, O. I. (2007). Breast cancer risk associated with BRCA1 and BRCA2 in diverse populations. *Nature Reviews Cancer*, *7*(12), 937–948. https://doi.org/10.1038/nrc2054

Ferlay, J., Soerjomataram, I., Dikshit, R., Eser, S., Mathers, C., Rebelo, M., Parkin, D. M., Forman, D., & Bray, F. (2015). Cancer incidence and mortality worldwide: Sources, methods and major patterns in GLOBOCAN 2012: Globocan 2012. *International Journal of Cancer*, *136*(5), E359–E386. https://doi.org/10.1002/ijc.29210

Fidler, M. M., Gupta, S., Soerjomataram, I., Ferlay, J., Steliarova-Foucher, E., & Bray, F. (2017). Cancer incidence and mortality among young adults aged 20–39 years worldwide in 2012: A population-based study. *The Lancet Oncology*, *18*(12), 1579–1589. https://doi.org/10.1016/S1470-2045(17)30677-0

Fredenberg, E., Svensson, B., Danielsson, M., Lazzari, B., & Cederström, B. (2011). Optimization of mammography with respect to anatomical noise; *SPIE Medical Imaging* (N. J. Pelc, E. Samei, & R. M. Nishikawa, Eds.; p. 796112). https://doi.org/10.1117/12.877985

Gagne, R. M., Boswell, J. S., Myers, K. J., & Peter, G. (2001). Lesion detectability in digital radiography; *Medical Imaging.* (L. E. Antonuk & M. J. Yaffe, Eds.; p. 316). https://doi.org/10.1117/12.430902

Gagne, R. M., Gallas, B. D., & Myers, K. J. (2005). Toward objective and quantitative evaluation of imaging systems using images of phantoms: Toward objective and quantitative evaluation of imaging systems. *Medical Physics*, *33*(1), 83–95. https://doi.org/10.1118/1.2140117

Gardner, K. E. (2006). *Early Detection: Women, Cancer, and Awareness Campaigns in the Twentieth-Century United States*. Univ of North Carolina Press.

Gethins, M. (2012). Breast Cancer in Men. *Journal of the National Cancer Institute*, *104*(6), 436–438. https://doi.org/10.1093/jnci/djs172

Ghoncheh, M., Pournamdar, Z., & Salehiniya, H. (2016). Incidence and Mortality and Epidemiology of Breast Cancer in the World. *Asian Pacific Journal of Cancer Prevention*, *17*(sup3), 43–46. https://doi.org/10.7314/APJCP.2016.17.S3.43

Giordano, S. H., Buzdar, A. U., & Hortobagyi, G. N. (2002). Breast Cancer in Men. *Annals of Internal Medicine*, *137*(8), 678–687. https://doi.org/10.7326/0003-4819-137-8-

200210150-00013

Golubicic, I., Borojevic, N., & Pavlovic, T. (2008). Risk factors for breast cancer: Is ionizing radiation among them? *Journal of Official Journal of the Balkan Union of Oncology*, *13*(4), 487–494.

Greg, H. (2007). Excel 2007 Workbook for Dummies. *Wiley. p. 296 Ff., 2nd ed.*

Groen, E. J., Elshof, L. E., Visser, L. L., Rutgers, E. J. Th., Winter-Warnars, H. A. O., Lips, E. H., & Wesseling, J. (2017). Finding the balance between over- and under-treatment of ductal carcinoma in situ (DCIS). *The Breast*, *31*, 274–283. https://doi.org/10.1016/j.breast.2016.09.001

Haus, A. G., Doi, K., Metz, C. E., & Bernstein, J. (1977). Image Quality in Mammography. *Radiology*, *125*(1), 77–85. https://doi.org/10.1148/125.1.77

Haus, A. G., & Yaffe, M. J. (2000). SCREEN-FILM AND DIGITAL MAMMOGRAPHY. *Radiologic Clinics of North America*, *38*(4), 871–898. https://doi.org/10.1016/S0033-8389(05)70207-4

Hassiotou, F., & Geddes, D. (2013). Anatomy of the human mammary gland: Current status of knowledge. *Clinical Anatomy*, *26*(1), 29–48. https://doi.org/10.1002/ca.22165

Hirko, K. A., Rocque, G., Reasor, E., Taye, A., Daly, A., Cutress, R. I., Copson, E. R., Lee, D.-W., Lee, K.-H., Im, S.-A., & Park, Y. H. (2022). The impact of race and ethnicity in breast cancer—Disparities and implications for precision oncology. *BioMed Central Medicine*, *20*(1), 72. https://doi.org/10.1186/s12916-022-02260-0

Hopkin's, M. (2020, July 20). *Normal Breast Development and Changes*. Retrieved on 10th June, 2022 from https://www.hopkinsmedicine.org/health/conditions-and-diseases/normal-breast-development-and-changes

Huda, W., Sajewicz, A. M., Ogden, K. M., & Dance, D. R. (2003). Experimental investigation of the dose and image quality characteristics of a digital mammography imaging system. *Medical Physics*, *30*(3), 442–448. https://doi.org/10.1118/1.1543572

Human Health Campus—Computed radiography and digital radiography. Retrieved September 15, 2022, from https://humanhealth.iaea.org/HHW/MedicalPhysics/DiagnosticRadiology/PerformanceTesting/Computedradiographyanddigitalradiography/index.html

International Atomic Energy Agency, (2016). *Human Health Campus—Computed radiography and digital radiography*. Retrieved on 10th July, 2022 from https://humanhealth.iaea.org/HHW/MedicalPhysics/DiagnosticRadiology/PerformanceTesting/Computedradiographyanddigitalradiography/index.html

International Atomic Energy Agency, (2009). *Human Health Series Number 2 Quality Assurance Program for Screen Film Mammography*. IAEA. Pg. 125-144

International Atomic Energy Agency, (2011). *Human Health Series Number 17 Quality Assurance Program for Screen Digital Mammography*. IAEA. Pg. 120-150

International Commission on Radiation Units and Measurements. (2009). *Mammography–Assessment of Image Quality*. ICRU, Oxford. UK: University Press.

ImageJ Manual. (2022). ImageJ. Retrieved on 11th October, 2022 from https://en.wikipedia.org/w/index.php?title=ImageJ&oldid=1107255617

Izdihar, K., Kanaga, K. C., Krishnapillai, V., & Sulaiman, T. (2015). Determination of Tube Output (kVp) and Exposure Mode for Breast Phantom of Various Thicknesses/Glandularity for Digital Mammography. *The Malaysian Journal of Medical Sciences*, *22*(1), 40–49.

Jatoi, I. (1999). Breast cancer screening. *The American Journal of Surgery*, *177*(6), 518–524. https://doi.org/10.1016/S0002-9610(99)00096-3

Johns Hopkins Medicine (2019). Anatomy of the Breast. Retrieved on 21st May, 2022 from Anatomy of the Breasts | Johns Hopkins Medicine

Kabat, G. C., Xue, X., Kamensky, V., Lane, D., Bea, J. W., Chen, C., Qi, L., Stefanick, M. L., Chlebowski, R. T., Wactawski-Wende, J., Wassertheil-Smoller, S., & Rohan, T. E. (2015). Risk of breast, endometrial, colorectal, and renal cancers in postmenopausal women in association with a body shape index and other anthropometric measures. *Cancer Causes & Control*, *26*(2), 219–229. https://doi.org/10.1007/s10552-014-0501-4

Kawashima, H., Ichikawa, K., Nagasou, D., & Hattori, M. (2017). X-ray dose reduction using additional copper filtration for abdominal digital radiography: Evaluation using signal difference-to-noise ratio. *Physica Medica*, *34*, 65–71. https://doi.org/10.1016/j.ejmp.2017.01.015

Kreiter, E., Richardson, A., Potter, J., & Yasui, Y. (2014). Breast cancer: Trends in international incidence in men and women. *British Journal of Cancer*, *110*(7), 1891–1897. https://doi.org/10.1038/bjc.2014.66

Lambe, M., Hsieh, C., Trichopoulos, D., Ekbom, A., Pavia, M., & Adami, H.-O. (1994). Transient Increase in the Risk of Breast Cancer after Giving Birth. *New England Journal of Medicine*, *331*(1), 5–9. https://doi.org/10.1056/NEJM199407073310102

Laprovitera, N., Riefolo, M., Ambrosini, E., Klec, C., Pichler, M., & Ferracin, M. (2021). Cancer of Unknown Primary: Challenges and Progress in Clinical Management. *Cancers*, *13*(3), 451. https://doi.org/10.3390/cancers13030451

Lemacks, M. R., Kappadath, S. C., Shaw, C. C., Liu, X., & Whitman, G. J. (2002). A dual-energy subtraction technique for microcalcification imaging in digital mammography-A signal-to-noise analysis. *Medical Physics*, *29*(8), 1739–1751. https://doi.org/10.1118/1.1494832

Lewin, J. M., D'Orsi, C. J., Hendrick, R. E., Moss, L. J., Isaacs, P. K., Karellas, A., & Cutter, G. R. (2002). Clinical Comparison of Full-Field Digital Mammography and Screen-Film Mammography for Detection of Breast Cancer. *American Journal of Roentgenology*, *179*(3), 671–677. https://doi.org/10.2214/ajr.179.3.1790671

Li, Y., Poulos, A., McLean, D., & Rickard, M. (2010). A review of methods of clinical image quality evaluation in mammography. *European Journal of Radiology*, *74*(3), e122–e131. https://doi.org/10.1016/j.ejrad.2009.04.069

Liu, L., Hao, X., Song, Z., Zhi, X., Zhang, S., & Zhang, J. (2021). Correlation between family history and characteristics of breast cancer. *Scientific Reports*, *11*(1), 6360. https://doi.org/10.1038/s41598-021-85899-8

Madigan, M. P., Ziegler, R. G., Benichou, J., Byrne, C., & Hoover, R. N. (1995). Proportion of Breast Cancer Cases in the United States Explained by Well-Established Risk Factors. *Journal of the National Cancer Institute*, *87*(22), 1681–1685. https://doi.org/10.1093/jnci/87.22.1681

Mammography. (2022). Retrieved on June, 2022 from https://en.wikipedia.org/w/index.php?title=Mammography&oldid=1096299099

Marchiori, D. (2004). *Clinical Imaging - E-Book: With Skeletal, Chest and Abdomen Pattern Differentials*. Elsevier Health Sciences.

Mayor, C. (2020). *Understand female breast anatomy*. Mayo Clinic. Retrieved from https://www.mayoclinic.org/healthy-lifestyle/womens-health/multimedia/breast-cancer-early-stage/sls-20076628 on June 2022

Meaney, P. M., Fanning, M. W., Li, D., Poplack, S. P., & Paulsen, K. D. (2000). A clinical prototype for active microwave imaging of the breast. *Transactions on Microwave Theory and Techniques*, *48*(11), 1841–1853. https://doi.org/10.1109/22.883861

Mehnati, P., Malekzadeh, R., & Sooteh, M. Y. (2019). Use of bismuth shield for protection of superficial radiosensitive organs in patients undergoing computed tomography: A literature review and meta-analysis. *Radiological Physics and Technology*, *12*(1), 6–25. https://doi.org/10.1007/s12194-019-00500-2

Mensah, A. C., Yarney, J., Nokoe, S. K., Opoku, S., & Clegg-Lamptey, J. N. (2016). Survival Outcomes of Breast Cancer in Ghana: An Analysis of Clinicopathological Features. *Open Access Library Journal*, *03*(01), 1–11. https://doi.org/10.4236/oalib.1102145

Monticciolo, D. L., Newell, M. S., Hendrick, R. E., Helvie, M. A., Moy, L., Monsees, B., Kopans, D. B., Eby, P. R., & Sickles, E. A. (2017). Breast Cancer Screening for Average-Risk Women: Recommendations from the ACR Commission on Breast Imaging. *Journal of the American College of Radiology*, *14*(9), 1137–1143. https://doi.org/10.1016/j.jacr.2017.06.001

Mørch, L. S., Skovlund, C. W., Hannaford, P. C., Iversen, L., Fielding, S., & Lidegaard, Ø. (2017). Contemporary Hormonal Contraception and the Risk of Breast Cancer. *New England Journal of Medicine*, *377*(23), 2228–2239. https://doi.org/10.1056/NEJMoa1700732

Moskowitz, C. S., Chou, J. F., Wolden, S. L., Bernstein, J. L., Malhotra, J., Friedman, D. N., Mubdi, N. Z., Leisenring, W. M., Stovall, M., Hammond, S., Smith, S. A., Henderson, T. O., Boice, J. D., Hudson, M. M., Diller, L. R., Bhatia, S., Kenney, L. B., Neglia, J. P., Begg, C. B., … Oeffinger, K. C. (2014). Breast Cancer After Chest Radiation Therapy for Childhood Cancer. *Journal of Clinical Oncology*, *32*(21), 2217–2223. https://doi.org/10.1200/JCO.2013.54.4601

Mother and Child, N. (2019). Benefits of Breastfeeding for the Infant/Young Child—Diarrhoea—Mother, Infant and Young Child Nutrition & Malnutrition—Feeding practices including micronutrient deficiencies prevention, control of wasting, stunting and underweight. Retrieved on 9th October, 2022 from https://motherchildnutrition.org/healthy-nutrition/about-essential-nutrition-actions/benefits-of-breastfeeding.html

Neitzel, U. (2005). Status and prospects of digital detector technology for CR and DR. *Radiation Protection Dosimetry*, *114*(1–3), 32–38. https://doi.org/10.1093/rpd/nch532

Noel, A., & Thibault, F. (2004). Digital detectors for mammography: The technical challenges. *European Radiology*, *14*(11), 1990–1998. https://doi.org/10.1007/s00330-004-2446-6

Nishikawa, R. M., & Yaffe, M. J. (1985). Signal-to-noise properties of mammographic film-screen systems: SNR properties of mammographic film-screen systems. *Medical Physics*, *12*(1), 32–39. https://doi.org/10.1118/1.595781

Ocean 2014. (2015). Quality *Assurance Software for Piranha and Cobia. User's Manual* (Version 3.7A).

Oeffinger, K. C., Fontham, E. T. H., Etzioni, R., Herzig, A., Michaelson, J. S., Shih, Y.-C. T., Walter, L. C., Church, T. R., Flowers, C. R., LaMonte, S. J., Wolf, A. M. D., DeSantis, C., Lortet-Tieulent, J., Andrews, K., Manassaram-Baptiste, D., Saslow, D., Smith, R. A.,

Brawley, O. W., & Wender, R. (2015). Breast Cancer Screening for Women at Average Risk: 2015 Guideline Update from the American Cancer Society. *314*(15), 1599–1614. https://doi.org/10.1001/jama.2015.12783

Ohene-Yeboah, M., & Adjei, E. (2012). Breast cancer in Kumasi, Ghana. *Ghana Medical Journal*, *46*(1), 8–13.

Page, D. L., Schuyler, P. A., Dupont, W. D., Jensen, R. A., Plummer, W. D., & Simpson, J. F. (2003). Atypical lobular hyperplasia as a unilateral predictor of breast cancer risk: A retrospective cohort study. *The Lancet*, *361*(9352), 125–129. https://doi.org/10.1016/S0140-6736(03)12230-1

Pandya, S., & Moore, R. G. (2011). Breast Development and Anatomy. *Clinical Obstetrics & Gynecology*, *54*(1), 91–95. https://doi.org/10.1097/GRF.0b013e318207ffe9

Parkin, D. M., & Fernández, L. M. G. (2006). Use of Statistics to Assess the Global Burden of Breast Cancer. *The Breast Journal*, *12*(s1), S70–S80. https://doi.org/10.1111/j.1075-122X.2006.00205.x

Pelengaris, S., Khan, M., & Evan, G. (2002). c-MYC: More than just a matter of life and death. *Nature Reviews Cancer*, *2*(10), 764–776. https://doi.org/10.1038/nrc904

Perry, N., Broeders, M., Wolf, C. de, Törnberg, S., Holland, R., & Karsa, L. von. (2008). European guidelines for quality assurance in breast cancer screening and diagnosis. Fourth edition—Summary document. *Oncology in Clinical Practice*, *4*(2), 74–86.

Personal History of Breast Cancer. Retrieved September 15, 2022, from https://www.breastcancer.org/risk/risk-factors/personal-history

Picon-Ruiz, M., Morata-Tarifa, C., Valle-Goffin, J. J., Friedman, E. R., & Slingerland, J. M. (2017). Obesity and adverse breast cancer risk and outcome: Mechanistic insights and strategies for intervention. *Cancer Journal for Clinicians. 67*(5), 378–397.

https://doi.org/10.3322/caac.21405

Pierce, J. P., Faerber, S., Wright, F. A., Rock, C. L., Newman, V., Flatt, S. W., Kealey, S., Jones, V. E., Caan, B. J., Gold, E. B., Haan, M., Hollenbach, K. A., Jones, L., Marshall, J. R., Ritenbaugh, C., Stefanick, M. L., Thomson, C., Wasserman, L., Natarajan, L., … Gilpin, E. A. (2002). A randomized trial of the effect of a plant-based dietary pattern on additional breast cancer events and survival: *Controlled Clinical Trials*, *23*(6), 728–756. https://doi.org/10.1016/S0197-2456(02)00241-6

Pinder, S. E. (2010). Ductal carcinoma in situ (DCIS): Pathological features, differential diagnosis, prognostic factors and specimen evaluation. *Modern Pathology*, *23*(S2), S8–S13. https://doi.org/10.1038/modpathol.2010.40

Pisano, E. D., Yaffe, M. J., Hemminger, B. M., Hendrick, R. E., Niklason, L. T., Maidment, A. D. A., Kimme-Smith, C. M., Feig, S. A., Sickles, E. A., & Braeuning, M. P. (2000). Current status of full-field digital mammography. *Academic Radiology*, *7*(4), 266–280. https://doi.org/10.1016/S1076-6332(00)80478-X

Pongnapang, N. (2005). Practical guidelines for radiographers to improve computed radiography image quality. *Biomedical Imaging and Intervention Journal*, *1*(2). https://doi.org/10.2349/biij.1.2.e12

Rezapour, J., Mostear, A., Tarighatnia, A., Falahati, F., Hosseini, S. M., Johal, G., Nader, N. D., Dastranj, L., & Abedi-Firouzjah, R. (2021). A trade-off between breast mean glandular dose and image quality in digital and conventional mammogram systems: A multicenter study. *Radioprotection*, *56*(3), 221–227. https://doi.org/10.1051/radiopro/2021017

Renganathan, L., Ramasubramaniam, S., Al-Touby, S., Seshan, V., Al-Balushi, A., Al-Amri, W., Al-Nasseri, Y., & Al-Rawahi, Y. (2014). What do Omani Women know about Breast Cancer Symptoms? *Oman Medical Journal*, *29*(6), 408–413.

https://doi.org/10.5001/omj.2014.110

Ronckers, C. M., Erdmann, C. A., & Land, C. E. (2004). Radiation and breast cancer: A review of current evidence. *Breast Cancer Research*, *7*(1), 21. https://doi.org/10.1186/bcr970

Sabel, M. S. (2009). Essentials of Breast Surgery: A Volume in the Surgical Foundations Series E-Book. *Elsevier Health Sciences*.

Samei, E., Dobbins, J. T., Lo, J. Y., & Tornai, M. P. (2005). A framework for optimising the radiographic technique in digital X-ray imaging. *Radiation Protection Dosimetry*, *114*(1–3), 220–229. https://doi.org/10.1093/rpd/nch562

Samei, E., Ranger N. T. and Delong, D.M.,. (2008). A comparative contrast-detail study of five medical displays. *Medical Physics*, 1358-1364. https://sci-hub.hkvisa.net/10.1118/1.2868780

Salvagnini, E., Pelc, N. J., Samei, E., Bosmans, H., Monnin, P., Nishikawa, R. M.; Struelens, L., Verdun, F., Marshall, N. W. (2011). *SPIE Proceedings [SPIE Medical Imaging - Lake Buena Vista, Florida. Medical Imaging 2011:* Physics of Medical Imaging - The use of detectability indices as a means of automatic exposure control for a digital mammography system. *79615J.* https://doi.org/10.1117/12.878119

Salvagnini, E., Bosmans, H., Struelens, L., & Marshall, N. W. (2015). Tailoring automatic exposure control toward constant detectability in digital mammography: Tailoring automatic exposure control toward constant detectability. *Medical Physics*, *42*(7), 3834–3847. https://doi.org/10.1118/1.492141

Schleede, S., Bech, M., Grandl, S., Sztrókay, A., Herzen, J., Mayr, D., Stockmar, M., Potdevin, G., Zanette, I., Rack, A., Weitkamp, T., & Pfeiffer, F. (2014). X-ray phase-contrast tomosynthesis for improved breast tissue discrimination. *European Journal of Radiology*, *83*(3), 531–536. https://doi.org/10.1016/j.ejrad.2013.12.005

Schueller, G., Riedl, C. C., Mallek, R., Eibenberger, K., Langenberger, H., Kaindl, E., Kulinna-Cosentini, C., Rudas, M., & Helbich, T. H. (2008). Image Quality, lesion detection, and diagnostic efficacy in digital mammography: Full-field digital mammography versus computed radiography-based mammography using digital storage phosphor plates. *European Journal of Radiology*, *67*(3), 487–496. https://doi.org/10.1016/j.ejrad.2007.08.016

Seeram, E. (2019). Full-Field Digital Mammography: Physical Principles and Quality Control, Full-Field Digital Mammography*: Digital Radiography*. pp. 111–123. Springer. https://doi.org/10.1007/978-981-13-3244-9_7

Siu, A. L. (2016). Screening for Breast Cancer: U.S. Preventive Services Task Force Recommendation Statement. *Annals of Internal Medicine*, *164*(4), 279. https://doi.org/10.7326/M15-2886

Sosu, E. K. (2018). *Optimization of radiological protection of patients undergoing mammography examination in Ghana* [Thesis, University of Cape Coast]. Retrieved on 12th May, 2022 from http://ir.ucc.edu.gh/jspui/handle/123456789/3432 Pg. 16-25

Sosu, E. K., Boadu, M., & Mensah, S. Y. (2018). Determination of dose delivery accuracy and image quality in full—Field digital mammography. *Journal of Radiation Research and Applied Sciences*, *11*(3), 232–236. https://doi.org/10.1016/j.jrras.2018.02.002

Thevi Rajendran, P., Krishnapillai, V., Tamanang, S., & Kumari Chelliah, K. (2012). Comparison of Image Quality Criteria between Digital Storage Phosphor Plate in Mammography and Full-Field Digital Mammography in the Detection of Breast Cancer. *The Malaysian Journal of Medical Sciences: 19*(1), 52–59.

Trickey, D., Siddaway, A. P., Meiser-Stedman, R., Serpell, L., & Field, A. P. (2012). A meta-analysis of risk factors for post-traumatic stress disorder in children and adolescents. *Clinical Psychology Review*, *32*(2), 122–138. https://doi.org/10.1016/j.cpr.2011.12.001

van den Brandt, P. A., Ziegler, R. G., Wang, M., Hou, T., Li, R., Adami, H.-O., Agnoli, C., Bernstein, L., Buring, J. E., Chen, Y., Connor, A. E., Eliassen, A. H., Genkinger, J. M., Gierach, G., Giles, G. G., Goodman, G. G., Håkansson, N., Krogh, V., Le Marchand, L., … Smith-Warner, S. A. (2021). Body size and weight change over adulthood and risk of breast cancer by menopausal and hormone receptor status: A pooled analysis of 20 prospective cohort studies. *European Journal of Epidemiology*, *36*(1), 37–55. https://doi.org/10.1007/s10654-020-00688-3

Wang, L. (2017). Early Diagnosis of Breast Cancer. *Sensors*, *17*(7), 1572. https://doi.org/10.3390/s17071572

Weir, H. K., Thun, M. J., Hankey, B. F., Ries, L. A. G., Howe, H. L., Wingo, P. A., Jemal, A., Ward, E., Anderson, R. N., & Edwards, B. K. (2003). Annual Report to the Nation on the Status of Cancer, 1975–2000, Featuring the Uses of Surveillance Data for Cancer Prevention and Control. *Journal of the National Cancer Institute*, *95*(17), 1276–1299. https://doi.org/10.1093/jnci/djg040

Western Missouri Medical Center (2018). *Understanding Breast Density*. Retrieved on 17th May, 2022 from https://wmmc.com/understanding-breast-density/

Wikipedia. (2022). Mammography. Wikipedia. Retrieved on 20th June, 2022 from, https://en.wikipedia.org/w/index.php?title=Mammography&oldid=1096299099

Wiredu, E. K., & Armah, H. B. (2006). Cancer mortality patterns in Ghana: A 10-year review of autopsies and hospital mortality. *BioMed Central Public Health*, *6*(1), 159. https://doi.org/10.1186/1471-2458-6-159

Willett, W. C., Tamimi, R., Hankinson, S. E., Hazra, A., Eliassen, A. H., & Colditz, G. A. (2014). Nongenetic factors in the causation of breast cancer. *Diseases of the Breast: Fifth Edition*. https://profiles.wustl.edu/en/publications/nongenetic-factors-in-the-causation-of-breast-cancer

Wohlfahrt, J. (2001). Risk of Late-stage Breast Cancer after a Childbirth. *American Journal of Epidemiology*, *153*(11), 1079–1084. https://doi.org/10.1093/aje/153.11.1079

World Health Organization (2000) *Cancer*. Retrieved September 15, 2022, from https://www.who.int/health-topics/cancer

Yaffe, M. J. (2010). Detectors for Digital Mammography. In U. Bick & F. Diekmann (Eds.), *Digital Mammography* (pp. 13–31). Springer Berlin Heidelberg. https://doi.org/10.1007/978-3-540-78450-0_2

Yaffe, M. J. (2011). Developing a quality control program for digital mammography: Achievements so far and challenges to come. Imaging in Medicine, 3(1), 123–133. https://doi.org/10.2217/iim.10.63

Yaffe, M. J., & Mainprize, J. G. (2011). Risk of radiation-induced breast cancer from mammographic screening. Radiology, 258(1), 98–105.

Yaffe, M. J., Bloomquist, A. K., Hunter, D. M., Mawdsley, G. E., Chiarelli, A. M., Muradali, D., & Mainprize, J. G. (2013). Comparative performance of modern digital mammography systems in a large breast screening program: Comparative performance of CR and DR mammography systems. *Medical Physics*, *40*(12), 121915. https://doi.org/10.1118/1.4829516

Yaffe, M. J., Bloomquist, A. K., Mawdsley, G. E., Pisano, E. D., Hendrick, R. E., Fajardo, L. L., Boone, J. M., Kanal, K., Mahesh, M., Fleischman, R. C., Och, J., Williams, M. B., Beideck, D. J., & Maidment, A. D. A. (2006). Quality control for digital mammography: Part II recommendations from the ACRIN DMIST trial: QC for digital mammography: Part II recommendations. *Medical Physics*, *33*(3), 719. https://doi.org/10.1118/1.2164067

Zhang, Q., Liu, L., Wang, F., Mu, K., & Yu, Z. (2012). The changes in female physical and childbearing characteristics in china and potential association with risk of breast cancer. *BioMed Central Public Health*, *12*(1), 368. https://doi.org/10.1186/1471-2458-12-368

Zucca-Matthes, G., Urban, C., & Vallejo, A. (2016). Anatomy of the nipple and breast ducts. *Gland Surgery*, *5*(1), 32. https://doi.org/10.3978/j.issn.2227-684X.2015.05.10

APPENDICES

APPENDIX A

ETHICAL CLEARANCE FROM ECBAS

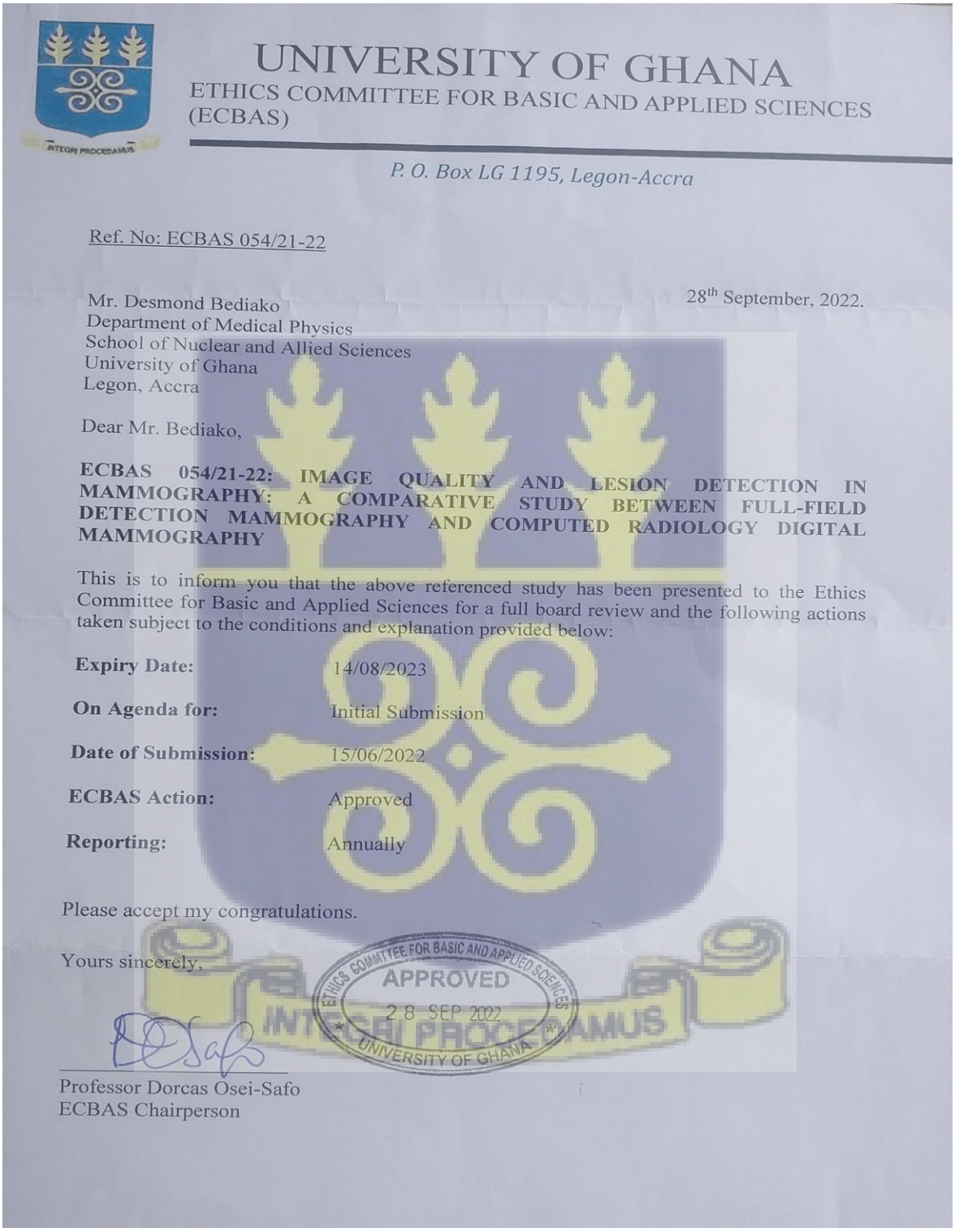

UNIVERSITY OF GHANA
ETHICS COMMITTEE FOR BASIC AND APPLIED SCIENCES
(ECBAS)

P. O. Box LG 1195, Legon-Accra

Ref. No: ECBAS 054/21-22

28th September, 2022.

Mr. Desmond Bediako
Department of Medical Physics
School of Nuclear and Allied Sciences
University of Ghana
Legon, Accra

Dear Mr. Bediako,

ECBAS 054/21-22: IMAGE QUALITY AND LESION DETECTION IN MAMMOGRAPHY: A COMPARATIVE STUDY BETWEEN FULL-FIELD DETECTION MAMMOGRAPHY AND COMPUTED RADIOLOGY DIGITAL MAMMOGRAPHY

This is to inform you that the above referenced study has been presented to the Ethics Committee for Basic and Applied Sciences for a full board review and the following actions taken subject to the conditions and explanation provided below:

Expiry Date:	14/08/2023
On Agenda for:	Initial Submission
Date of Submission:	15/06/2022
ECBAS Action:	Approved
Reporting:	Annually

Please accept my congratulations.

Yours sincerely,

ETHICS COMMITTEE FOR BASIC AND APPLIED SCIENCES
APPROVED
28 SEP 2022
UNIVERSITY OF GHANA

Professor Dorcas Osei-Safo
ECBAS Chairperson

APPENDIX B

ETHICAL CLEARANCE FROM 37 MILITARY HOSPITAL

Institutional Review Board
37 Military Hospital
Neghelli Barracks
ACCRA

Tel: 059 1759506
Email: irbmilhosp@gmail.com

29 July 2022

ETHICAL CLEARANCE

37MH-IRB/MAS/IPN/642/22

On 29 July 2022 the 37 Military Hospital (37MH) Institutional Review Board (IRB) approved your protocol.

TITLE OF PROTOCOL: **Image Quality and Lesion Detection in Mammography: A Comparative Study between Full-Field Digital Mammography and Computed Radiography Digital Mammography**

PRINCIPAL INVESTIGATOR: **Desmond Bediako**

Please note that a final review report must be submitted to the Board at the completion of the study.

Please report all serious adverse events related to this study to 37MH-IRB within seven (7) days verbally and fourteen (14) days in writing.

This certificate is valid till 28 July 2023.

DR EDWARD ASUMANU
(37MH-IRB, Vice Chairman)

INSTITUTIONAL REVIEW BOARD
29 JUL 2022
37 MILITARY HOSPITAL ACCRA

Cc: Brig Gen AG Bugri
Commander, 37 Military Hospital

INTEGRI PROCEDAMUS

APPENDIX C

DATA FOR ESTIMATING COMPRESSION THICKNESS

Mammography Systems	PMMA Thicknesses (mm)					
	20		45		70	
	Measured Thickness (mm)	Displaced Thickness (mm)	Measured Thickness (mm)	Displaced Thickness (mm)	Measured Thickness (mm)	Displaced Thickness (mm)
A	20	21	43	45	67	68
B	19	21	48	45	73	70
C	19	21	44	46	67	68
D	19	20	44	46	70	71
E	16	20	42	43	68	70

APPENDIX D

DATA FOR ESTIMATING COMPRESSION FORCE

COMPRESSION MODE	AUTOMATIC COMPRESSION		MANUAL COMPRESSION	
MAMMOGRAPHY SYSTEMS	MEASURED FORCE (N)	DISPLAYED FORCE (N)	MEASURED FORCE (N)	DISPLAYED FORCE (N)
A	116	112	123	120
B	103	100	91	89
C	115	110	127	122
D	99	90	72	68
E	101	99	107	104

APPENDIX E

DATA FOR ESTIMATING COMPRESSION ALIGNMENT

MAMMOGRAPHY SYSTEMS	Compression Alignment (mm)			
	Rear Left	Front Left	Rear Right	Front Right
			20 mm	
A	21	21	21	21
B	21	21	22	21
C	20	22	21	22
D	21	21	21	21
E	23	24	24	23
			45 mm	
A	47	46	46	47
B	43	43	42	43
C	46	47	47	46
D	47	46	47	45
E	46	46	46	46
			70 mm	
A	70	71	70	71
B	67	66	67	67
C	71	71	71	71
D	70	70	71	71
E	73	72	72	72

APPENDIX F

DATA FOR ESTIMATING KVP ACCURACY AND REPEATABILITY

MAMMOGRAPHY SYSTEM	A	B	C	D	E
kVp1	39.17	28.80	28.09	28.50	28.62
kVp2	39.18	28.73	28.21	28.45	28.60
Repeatability Difference (%)	0.03	0.24	0.43	0.18	0.07
kVp3	39.27	28.69	28.20	28.59	28.60
kVp4	39.22	28.77	28.27	28.53	28.64
kVp5	39.31	28.78	28.19	28.52	28.59
Mean KVp	39.23	28.75	28.19	28.52	28.61
Standard Deviation	0.06	0.04	0.06	0.05	0.02
Repeatability COV (%)	0.15	0.15	0.23	0.18	0.07
Nominal KVp – Mean kVp	0.77	0.75	0.19	0.52	0.61

APPENDIX G

DATA FOR ESTIMATING THE OUTPUT REPEATABILITY AND LINEARITY

Mammography Systems	mAs	Expo. 1	Expo. 2	Expo. 3	Expo. 4	Expo. 5	Mean Value	Standard Deviation	Repeatability Difference (%)	Repeatability COV (%)	Output (Y_1)	Output (Y_2)	Output (Y_3)	Linearity (L)
	40	1.695	1.726	1.727	1.728	1.729	1.721							
A	80	3.465	3.462				3.464	0.015	0.17	0.85	0.045	0.043	0.043	0.02
	120	5.416	5.406				5.411							
	40	1.13	1.322	1.134	1.132	1.131	1.132							
B	80	2.23	2.23				2.23	0.001	0.09	0.13	0.028	0.028	0.028	0.163
	120	3.471	3.475				3.473							
	40	3.579	3.578	3.583	3.581	3.585	3.581							
C	80	7.195	7.191				7.191	0.003	0.2	0.08	0.09	0.09	0.09	0.113
	120	11.72	11.71				11.715							
	40	4.563	3.808	4.207	4.512	4.588	4.336							
D	80	3.584	9.104				6.344	0.332	0.2	0.08	0.105	0.079	0.108	0.14
	120	11	14.24				12.62							
	40	3.944	3.933	3.929	3.925	3.934	3.933							
E	80	8.434	8.433				8.434	0.007	0.03	0.18	0.107	0.105	0.098	0.007
	120	13.91	13.9				13.905							

APPENDIX H

DATA FOR ESTIMATING HALF VALUE LAYER

Mammography system	Exposures	Constant	Minimum HVL	Maximum HVL	Calculated HVL
A	1.714 1.503 1.324 1.172 1.039 0.835	0.3	0.31	0.58	0.58
B	1.132 0.885 0.796 0.659 0.601 0.534	0.3	0.31	0.58	0.55
C	3.585 3.027 2.577 2.211 1.904 1.77	0.22	0.31	0.5	0.45
D	4.045 3.774 1.821 4.033 3.321 2.787	0.12	0.31	0.4	0.2
E	2.333 1.962	0.12	0.31	0.5	0.41

APPENDIX I

DATA FOR ESTIMATING THE TIMER AND KVP LINEARITY

Mammography systems	kVp	Exposures	$(kVp)^2$	Exposure Time	R - Value	R^2
	20	0.464	400	401.6		
	22	0.696	484	418.5		
A	24	1.034	576	439.3	0.985340802	0.970896497
	26	1.373	676	472.1		
	28	1.733	784	520.9		
	23	0.582	529	690.0		
	25	0.818	625	675.5		
B	27	1.029	729	663.1	-0.99559712	0.991213628
	29	1.235	841	646.5		
	31	1.438	961	622.6		
	20	0.887	400	520.4		
	22	1.327	484	523.1		
C	24	1.957	576	526.5	0.999476323	0.99895292
	26	2.715	676	530.4		
	28	4.523	784	534.5		
	22	1.643	484	412.0		
	24	2.654	576	422.1		
D	26	3.537	676	434.1	0.996064414	0.992144317
	28	4.604	784	451.3		
	30	5.637	900	470.3		
	20	1.43	400	552.5		
	22	1.641	484	506.9		
E	24	2.39	576	475.3	-0.98786545	0.975878137
	26	3.079	676	432.6		
	28	3.915	784	412.0		

APPENDIX J

DATA FOR ESTIMATING THE TIMER REPEATABILITY

Mammography systems	Exposure Time	Average Time	Standard Deviation	Repeatability Difference (%)	Repeatability COV (%)
	547.5				
	547.5				
A	548.0	547.42	0.39623226	0.182815356	0.07238
	547.0				
	547.1				
	691.1				
	689.5				
B	690.0	689.12	1.62696036	0.59679767	0.2360925
	687.0				
	688.0				
	538.0				
	537.0				
C	537.5	537.30	0.4472136	0.18621974	0.0832335
	537.0				
	537.0				
	412.0				
	422.1				
D	421.1	445.56	38.5111412	21.1893204	8.6433121
	473.3				
	499.3				
	414.0				
	412.5				
E	413.0	413.30	0.67082039	0.36363636	0.1623083
	413.0				
	414.0				

APPENDIX K

DATA FOR ESTIMATING LESION DETECTION IN ACR-MAP

Mammography Systems	INSERTS	EVALUATIONS	26/32	28/40	29/50	30/90	32/130
A	FIBER	Totally Visual (1)	2	3	3	3	5
		Partially Visual (0.5)	2	3	2	3	2
		Less than half (0)	2	0	1	0	0
	SPECKS	Four or more Visual (1)	2	2	3	3	3
		two/three Visual (0.5)	3	2	2	2	2
		Less than 2 Visual (0)	2	1	1	0	0
	MASS	Totally Visual (1)	2	2	3	4	4
		Partially Visual (0.5)	1	2	1	1	1
B	FIBER	Totally Visual (1)	2	3	3	3	5
		Partially Visual (0.5)	3	2	2	3	1
		Less than half (0)	1	2	1	0	0
	SPECKS	Four or more Visual (1)	2	2	2	3	3
		two/three Visual (0.5)	3	3	3	2	2
		Less than 2 Visual (0)	2	2	0	0	0
	MASS	Totally Visual (1)	2	2	3	4	4
		Partially Visual (0.5)	2	2	2	1	1
C	FIBER	Totally Visual (1)	2	3	2	3	4
		Partially Visual (0.5)	2	1	1	2	1
		Less than half (0)	2	2	3	1	1
	SPECKS	Four or more Visual (1)	2	3	3	3	3
		two/three Visual (0.5)	1	0	2	2	2
		Less than 2 Visual (0)	2	2	0	0	0
	MASS	Totally Visual (1)	1	2	3	2	3
		Partially Visual (0.5)	2	1	1	2	2
D	FIBER	Totally Visual (1)	1	1	2	3	3
		Partially Visual (0.5)	1	1	3	2	2
		Less than half (0)	4	4	1	1	0
	SPECKS	Four or more Visual (1)	0	0	1	3	3
		two/three Visual (0.5)	2	3	2	2	1
		Less than 2 Visual (0)	4	3	3	1	0
	MASS	Totally Visual (1)	0	2	2	2	2
		Partially Visual (0.5)	2	3	4	2	4
E	FIBER	Totally Visual (1)	2	3	3	4	4
		Partially Visual (0.5)	2	5	2	2	1
		Less than half (0)	2	2	1	0	1
	SPECKS	Four or more Visual (1)	2	2	3	2	2
		two/three Visual (0.5)	3	1	1	2	2
		Less than 2 Visual (0)	2	2	1	0	0
	MASS	Totally Visual (1)	2	1	2	3	4
		Partially Visual (0.5)	1	3	3	2	1

APPENDIX L

DATA FOR ESTIMATING THE SIGNAL-TO-NOISE-RATIO

PMMA THICKNESS (mm)	20 mm		45 mm		70 mm	
	MPV	STDEV	MPV	STDEV	MPV	STDEV
			SYSTEM A			
AL-PMMA ROI 1	**198.67**	**3.98**	**226.05**	**1.99**	**192.18**	**1.86**
PMMA ROI 2	155.18	5.34	204.14	2.85	171.18	3.11
PMMA ROI 3	152.28	4.19	203.23	2.78	178.53	3.21
PMMA ROI 4	148.88	4.29	205.99	2.48	181.23	3.29
PMMA ROI 5	139.35	4.26	194.90	2.96	169.31	3.79
			SYSTEM B			
AL-PMMA ROI 1	**186.00**	**4.47**	**209.18**	**1.88**	**251.77**	**4.01**
PMMA ROI 2	148.42	4.94	198.12	3.21	242.80	3.21
PMMA ROI 3	139.63	4.07	180.73	2.11	230.77	3.91
PMMA ROI 4	121.38	4.99	181.43	2.91	231.25	3.04
PMMA ROI 5	101.06	5.34	180.31	1.79	230.77	3.66
			SYSTEM C			
AL-PMMA ROI 1	**214.02**	**2.04**	**4183.50**	**181.44**	**5154.78**	**284.58**
PMMA ROI 2	168.39	4.28	3132.49	141.58	4395.69	258.45
PMMA ROI 3	199.98	2.63	2947.94	178.93	4326.97	277.33
PMMA ROI 4	165.60	3.55	2919.80	142.09	4622.66	261.07
PMMA ROI 5	195.35	2.16	3113.81	144.92	4555.62	235.60
			SYSTEM D			
AL-PMMA ROI 1	**203.18**	**1.96**	**4370.19**	**235.29**	**219.48**	**6.03**
PMMA ROI 2	183.12	3.11	3659.91	221.91	208.19	6.71
PMMA ROI 3	183.63	2.71	3940.61	204.73	215.30	6.07
PMMA ROI 4	181.83	2.89	3938.31	216.81	216.01	6.59
PMMA ROI 5	183.37	2.89	3701.25	226.98	211.28	7.53
			SYSTEM E			
AL-PMMA ROI 1	**131.18**	**1.91**	**231.31**	**2.90**	**4890.19**	**235.29**
PMMA ROI 2	111.19	2.34	215.63	3.65	3659.91	221.91
PMMA ROI 3	119.27	1.89	219.80	3.71	3940.61	204.73
PMMA ROI 4	120.60	1.70	212.51	3.13	3938.31	216.81
PMMA ROI 5	112.37	1.70	191.32	3.28	3701.25	226.98